List of papers published/ to be published

1. Synthesis and properties of copper (II), oxovanadium (IV) and gadolinium (III) complexes derived from polar Schiff's bases

Lopamudra Chakraborty, Nirmalangshu Chakraborty, Atiqur Rahman Laskar, Manoj Kumar Paul, Nandiraju V.S. Rao, Journal of Molecular Structure,1002, (2011) ,135–144.

2. Synthesis, mesomorphic and photo-physical properties of few *d*- and *f*-block metals coordinated to polar Schiff's bases

Lopamudra Chakraborty , Nirmalangshu Chakraborty , Trirup Dutta Choudhury , B. V. Phani Kumar , Asit B. Mandal and Nandiraju V.S. Rao, *Liquid Crystals*, Vol. 39, No. 5, May 2012, 655–668.

3. Unusual Smectic Cluster Formation in the Nematic Phase in a Hockey-stick-shaped Four-Ring Compound

Lopamudra Chakraborty, Nirmalangshu Chakraborty, Dipika Debnath Sarkar, Nandiraju V.S. Rao, Satoshi Aya, K.V.Le, Ken Ishikawa, Hideo Takezoe (submitted to JMC).

4. Stripe domains in a nearly homeotropic nematic liquid crystal, and temperature dependence of elastic constants in the nematic phase of binary mixtures comprised of rod-like and bent-core molecules

Nirmalangshu Chakraborty, Golam Mohiuddin and Nandiraju V S Rao, Khoa Van Le, Ken Ishikawa and Hideo Takezoe (communicated to Soft Matter).

5. Synthesis of achiral four-ring unsymmetrically substituted toluene derived liquid crystals with a polar end group

Dipika Debnath Sarkar, Rahul Deb, Nirmalangshu Chakraborty and Nandiraju V S Rao (accepted in Liquid Crystal,2012, in press).

6. Fluorine substituted four ring bent core molecules with polar ordered B7 phases

Nirmalangshu Chakraborty, Golam Mohiuddin, Manoj K Paul and Nandiraju V S Rao (submitted to Chem. Mater.).

Liquid Crystals
Publication details, including instructions for authors and subscription information:
http://www.tandfonline.com/loi/tlct20

Synthesis, mesomorphic and photo-physical properties of few d- and f- block metals coordinated to polar Schiff's bases

Lopamudra Chakraborty [a], Nirmalangshu Chakraborty [a], Trirup Dutta Choudhury [a], B.V.N. Phani Kumar [b], Asit Baran Mandal [b] & Nandiraju V.S. Rao [a]

[a] Chemistry Department, Assam University, Assam, India

[b] Council of Scientific and Industrial Research (CSIR)-Central Leather Research Institute, Chennai, India

Available online: 21 Mar 2012

To cite this article: Lopamudra Chakraborty, Nirmalangshu Chakraborty, Trirup Dutta Choudhury, B.V.N. Phani Kumar, Asit Baran Mandal & Nandiraju V.S. Rao (2012): Synthesis, mesomorphic and photo-physical properties of few d- and f- block metals coordinated to polar Schiff's bases, Liquid Crystals, 39:5, 655-668

To link to this article: http://dx.doi.org/10.1080/02678292.2012.669854

Liquid Crystals,
Vol. 39, No. 5, May 2012, 655–668

Taylor & Francis
Taylor & Francis Group

Synthesis, mesomorphic and photo-physical properties of few *d*- and *f*- block metals coordinated to polar Schiff's bases

Lopamudra Chakraborty[a], Nirmalangshu Chakraborty[a], Trirup Dutta Choudhury[a], B.V.N. Phani Kumar[b], Asit Baran Mandal[b] and Nandiraju V.S. Rao[a]*

[a]*Chemistry Department, Assam University, Assam, India;* [b]*Council of Scientific and Industrial Research (CSIR)–Central Leather Research Institute, Chennai India*

(*Received 28 October 2011; final version received 22 February 2012*)

The synthesis, liquid crystalline and optical properties of polar Schiff's bases, viz. N-(4-*n*-hexadecyloxysalicylidene)-4′-substituted anilines with methyl, nitro and cyano substituents in the 4-position of N-aryl moiety and their *d*- and *f*-block metal complexes, are presented. The polar ligands exhibited a smectic A phase, while methyl homologue exhibited a nematic phase. The majority of the complexes exhibited a smectic A phase with some of them exhibiting smectic E phases. The ultraviolet-visible and photo-physical properties of the ligands and complexes are also discussed.

Keywords: mesomorphism; polar Schiff's base; fluorescence; metallomesogens

1. Introduction

Soft fluid materials possessing magnetic, electronic and luminescent properties have received considerable attention recently because of their potential technological applications. Metal-containing liquid crystals (LCs), viz. metallomesogens [1–14], are one of the prominent candidates for such applications. Metallomesogens can be designed such that a soft fluid property can be generated by designing a proper organic ligand that can be coordinated to a metal ion that contributes to the electronic, magnetic and optical properties [12, 13]. Schiff base ligands consisting of two phenyl rings with alkyl(oxy) substituents linked with an imine linkage, viz. N-(4-*n*-alkoxysalicylidene)-4′-*n*-alkylanilines, not only exhibit rich polymesomorphism, but are also excellent coordinating ligands through oxygen and nitrogen atoms [15–34]. The majority of the metallomesogens described in literature contains the *d*-block metal ions, in particular Cu(II), Ni(II), VO(IV), Pd(II) or Pt(II), as the central metal ion. However, the reported coordination of *f*-block lanthanides ions with Schiff base ligands **L1–L4** (Figure 1) is limited to N-(4-*n*-alkoxysalicylidene)-4′-*n*-alkylamines [14, 28–36] and phthalocyanines [37]. In last two decades several calamitic bidentate salicylideneimines [*n*OPh(OH)m_{ali}], possessing N-aliphatic moiety-based lanthanide complexes viz. lanthanidomesogens are reported [14, 28–34]. However, the efforts to coordinate *f*-block metals with the N-(4-*n*-alkoxysalicylidene)-4′-*n*-alkylanilines, that is, ligands with an aryl moiety [31, 32] on the nitrogen atom of the central bridging imine group have been unsuccessful. The difference in basicity of the nitrogens of N-alkyl and N-aryl imines of the ligand promotes the formation of a zwitter ion, which led to the coordination of the zwitter ionic N-alkyl imines only to form the lanthanide complexes, but it is not realised with aromatic imines. Recently, it has been reported that N, N′-aromatic donor [35] (Figure 2), viz. 4,7-disubstitttuted phenanthroline (**L5** and **L6**) or 4,4′-dimethoxy-2,2′-bipyridine (**L7**), coordination with

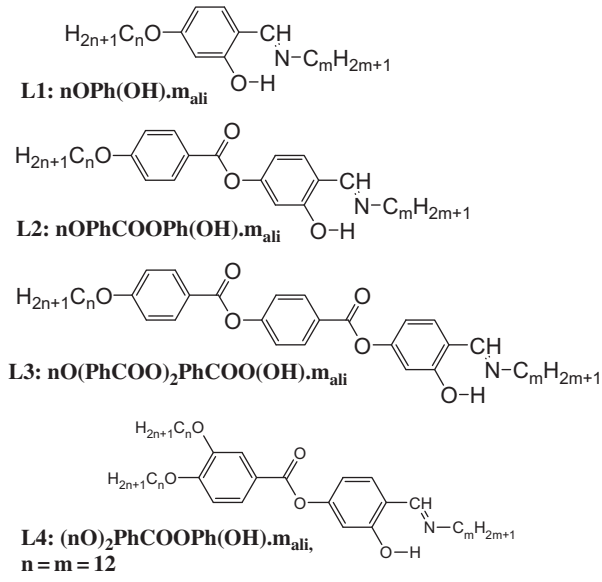

Figure 1. Molecular structure of Schiff's base ligands studied extensively for complexation [16, 26–32].

*Corresponding author. Email: drnvsrao@gmail.com

ISSN 0267-8292 print/ISSN 1366-5855 online

http://dx.doi.org/10.1080/02678292.2012.669854
http://www.tandfonline.com

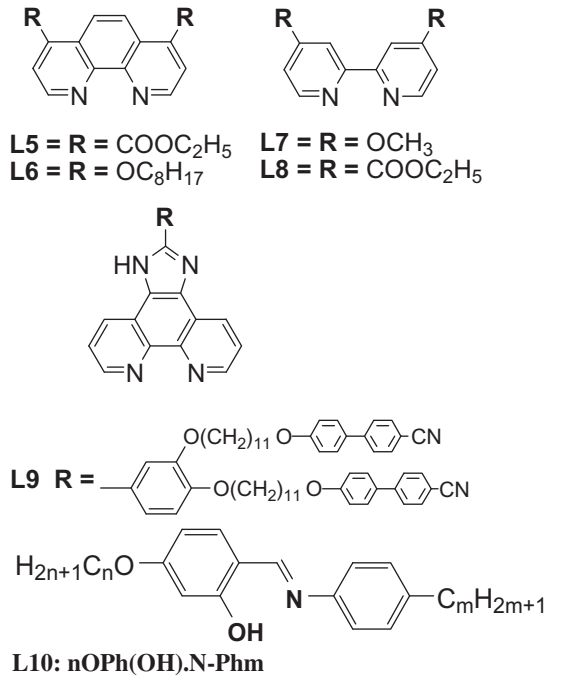

Figure 2. Molecular structure of N, N′-aromatic donors for complexation [33, 34].

the lanthanide ions is successful, while diethyl-2,2′-bipyridine-4,4′-dicarboxylate (**L8**) does not participate in coordination. Hence, it has been established that an electronic destabilisation of the ester groups on the aromatic bipyridine core, which is associated with a more flexible conformation with respect to the phenanthroline, makes this ligand incompatible for chelation with a lanthanide ion of any size . In fact, the influence of the substituents on the basicity and the coordination ability of the N, N′-aromatic ligands, viz. 4,4′-dimethoxy-2,2′-bipyridine, (**L7**) the bipyridine bearing a methoxy group in the 4,4′ position, produced high yields of the complexes, reflecting the dramatically enhanced activation towards coordination. However, modification of the phenanthroline ligand (**L9**) in 5,6-positions fused with a substituted imidazo ring [36] led to the realisation of nematic phase. Recently, we were successful in the complexation of salicylideneimines possessing N-aryl moiety [38–40].

Hence, the design and synthesis of lanthanide-containing LCs, viz. salicylideneimine-based promesogenic ligands, with a polar group attached to an aryl moiety on the nitrogen atom of the central bridging imine group in order to coordinate with *f*-block metals presents a special experimental challenge. Our previous attempts were successful in reporting the complexation of different lanthanide ions with N-(4-*n*-alkoxysalicylidene)-4′-*n*-alkylanilines, **L10** [38–40]. The lanthanide complexes in general exhibited a smectic A (SmA) phase, but some of them exhibited columnar phases [16, 40, 41], depending on the percentile component of aliphatic chains. In continuation of earlier work [38–40], we report here the complexation of different lanthanide (III) ions, viz. Gd, Sm and Pr, with N-(4-*n*-hexadecyloxysalicylidene)-4′-substituted-anilines, the substituent being a methyl group or a polar cyano or nitro group in the N-aryl moiety. The characterisation of the ligands, as well as complexes for mesomorphism and their spectroscopic characteristics, are presented.

2. Experimental details

All the chemicals were procured from M/s Alfa Aesar, Aldrich or Tokyo Kasei Kogyo Co. Ltd. The solvents and reagents are of AR grade and were distilled and dried before use. Micro analysis of C, H and N elements were determined on a Carlo-Erba 1106 elemental analyser. Infrared (IR) spectra were recorded on a Perkin-Elmer L 120-000A spectrometer (ν_{max} in cm^{-1}) in KBr pellets. The proton (^1H) nuclear magnetic resonance spectra were recorded either on JEOL ECA-500 (500 MHz) multinuclear spectrometer or a Bruker DPX-400 spectrometer in $CDCl_3$ (chemical shift in δ) solution with tetramethylsilane (TMS) as the internal standard. Chemical shifts are reported in parts per million. The phase transition temperatures and associated enthalpies were recorded using differential scanning calorimetry (DSC; Perkin-Elmer Pyris-1 system). The liquid crystalline properties of the different phases exhibited by the ligands and complexes were observed and characterised using a polarising microscope (Nikon optiphot-2-pol attached with hot and cold stage HCS302, with an STC200 temperature controller configured for HCS302 from INSTEC Inc., USA). Ultraviolet-visible (UV-Vis) absorption spectra of the compounds in $CHCl_3$ at different concentrations were recorded on a Shimadzu UV-1601PC spectrophotometer (λ_{max} in nm). Fluorescence spectra were recorded with a Shimadzu RF-5301PC Spectroflouorometer with 150 W xenon lamp as the excitation source.

3. Results and discussion

The synthesis of ligands, viz. N-(4-*n*-hexadecyloxysali cylidene)-4′-substituted-(methyl, cyano and nitro)-anilines (hereafter abbreviated as 16O(OH)X where X = Me, CN, NO_2) and their Cu(II), VO(IV) (*d*-block) complexes and Gd(III), Sm(III) and Pr(III) (*f*-block) complexes as depicted in Scheme 1, was carried out following the procedure described in Section 2.

Elemental analysis of the ligands and copper (II) and oxovanadium (IV) complexes were consistent with their proposed structures. Elemental analysis of the

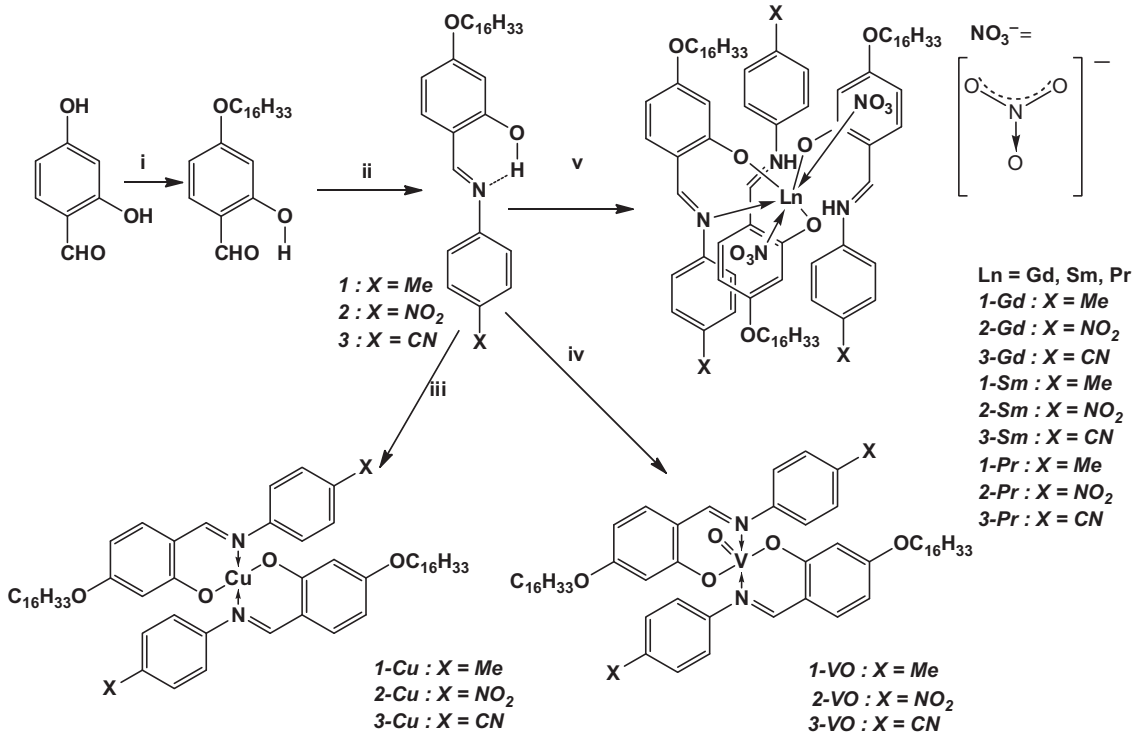

Scheme 1. i: $C_{16}H_{33}Br$, $KHCO_3$, KI, dry acetone, reflux, 40h, ii. 1 = 4-toluidine, 2 = 4-nitroaniline, 3 = 4-cyanoaniline, glacial AcOH, absolute EtOH, Reflux, 4h, iii. $Cu(OAc)_2$. H_2O, EtOH, Reflux, 4h; iv. $VOSO_4$ ċ $5H_2O$, MeOH, TEA, Reflux, 4h; v. $Gd(NO_3)_3$;/$Sm(NO_3)_3$;/$Pr(NO_3)_3$; Acetonitrile, Reflux, 4h for the sake of clarity the coordination of oxygen atoms of nitrate ion is shown through nitrate ions.

Table 1. Electrical conductivity of the compound 1, its complex and $Gd(NO_3)_3.6H_2O$. The concentration is 1×10^{-3} M.

	Molar conductivity ($S.cm^2.mol^{-1}$)		
Compound	N,N'-dimethylformamide	Ethanol	Acetonitrile
1	13	12	8
1-Gd	161	81	175
$Gd(NO_3)_3.6H_2O$	205	83	30

Ln(III) complexes [(Gd(III), Sm(III), Pr(III)] revealed the composition as $\{[Ln(LH)_2L](NO_3)_2\}$. The conductivity values (Table 1) inferred that the ligand is a non-electrolyte. The gadolinium complex is found to be a 2:1 electrolyte with the participation of two nitrate ions from the outer coordination sphere [42] supporting the elemental analysis data. Even though the exact stoichiometry of the lanthanide complexes is found to be difficult to confirm due to the relatively large molecular weight of the complex, the IR studies that are described below supported the molecular structure reflected from elemental analysis results. The formation of ligands was also confirmed by proton nuclear magnetic resonance (^{1}H-NMR) with a sharp singlet at ~8.5 ppm appearing for the imine proton. The formation of the complexes was confirmed from the Fourier transform infrared (FTIR) spectra. The room temperature IR spectra of the ligands exhibited a characteristic imine band of $\nu_{(CH=N)}$ (~1622–1627cm^{-1}), which shifted to lower frequencies for the copper(II) (1608cm^{-1}) and oxovanadium (IV) (1608–1610 cm^{-1}) complexes. This reflected the azomethine N atom participation in metal–nitrogen bond formation. The oxovanadium (IV) complexes exhibit a stretching band at ~966–987 cm^{-1} assigned to $\nu_{(V\text{-}O)}$, suggesting that these complexes possess a monomeric structure [43–48]. Further, for Ln(III) complexes of **1-Gd**, **2-Gd**, **3-Gd**, **1-Sm**, **3-Sm** and **3-Pr**, two characteristic absorption bands of the imine linkage appeared at 1639 and 1602 cm^{-1}, because of the zwitter ionic structure of the complex [40, 49]. The IR bands for **1-Pr**, **2-Pr** and **2-Sm** appeared at 1643 and 1602 cm^{-1}. The peak for the cyano group for all the ligands and complexes appeared at 2222 cm^{-1} and no appreciable shift of this band was observed upon complexation. Of the two stretching frequencies of imine linkage in the lanthanide complexes, one is the elongated stretching, viz. exactly opposite with an increase in the imine H**C**=**N** stretching vibration of the complex (at 1643–1639 cm^{-1}) in the IR spectra when compared to the stretching vibration in the free Schiff base ligand, while the other one is a compressed imine bond

appearing at a lower value of 1602 cm^{-1}. The vibration frequency at (1643–1639 cm^{-1}) is due to the complexation of the oxygen atom with the rare earth ion. The recorded vibrations in the region at 1465, 1290, 1118 and 825 cm^{-1} reflected the vibrations of coordinated modes of the nitrate group in bidentate fashion, apart from the observed vibration at ~1384 cm^{-1} of the free nitrate group. These values are in good agreement with the previous report [40]. Hence, the composition of newly synthesised lanthanide complexes has been considered as $\{[Ln(LH)_2L](NO_3)_2\}$, where LH = 16O(OH)X

4. Photo-physical studies

The formation of complexes can also be confirmed by UV-visible spectroscopy, as shown in Figure 3. For the cyano-substituted ligand (Figure 3(a)), two high-energy peaks at 279 and 316 nm appeared due to different types of π-π* transitions in the substituted benzene ring, whereas the shoulder that appeared at ~350 nm reflected the π-π* transition of the (-C=N-) bond of the imine group. In the gadolinium (III) complex, the π-π* transition of the benzene ring shifted towards higher energy (Figure 3(b)) and appeared at 246 and 303 nm, respectively, but no appreciable shift was observed for the π-π* transition of the imine group, which appeared at 354 nm. The only observed difference is the intensity of the peaks, which is much higher in complexes than in ligands. For copper complexes these three bands appeared at ~248 and ~309 nm, and an extra band appeared at ~369 nm due to ligand-to-metal charge transfer (LMCT). UV spectra of nitro- and methyl-substituted ligands and complexes exhibited similar results. Table 2 collects the spectroscopic results and photo-physical data for the ligands and some of the complexes.

Fluorescence spectroscopy represents an appropriate technique for investigating the structural properties of fluorophores in a liquid system [50]. Polarity of the solvent has a profound effect in the emission spectra of the compounds. In general, polar solvents stabilise the excited state by reorienting the solvent dipole (relaxation) in the excited state. This relaxation effect is much larger in the case of polar molecules than for non-polar ones [50]. Emission generally occurs from the first excited electronic state and hence it should be independent of the excited wavelength. The study of luminescence in emissive compounds is of fundamental interest, and they also have potential applications in optical amplifiers, organic light-emitting diodes (OLEDs), etc. Emission spectra of the ligand and complexes were studied in both solution and solid states to investigate the fluorescence property of these systems. All the ligands **1**–**3** exhibited emission spectra. All the lanthanide complexes exhibited emission spectra, but copper and oxovanadium complexes did not exhibit the emission property. In copper and oxovanadium complexes, no emission was observed due to free orientation of the emission dipole.

The methyl and nitro-substituted ligands (**1** and **2**, respectively), as well as their lanthanide complexes, exhibited only one emission peak above 500 nm when excited at 345 nm. However, the cyano-substituted ligand **3** exhibited a high-intensity emission peak at 430 nm when excited at 280 nm, with a large stoke shift of 152 nm. Further excitation at 300–340 nm gave two emission peaks at 430 and 526 nm. This dual emission spectrum [51] was observed either due to formation of different types of conformers or due to emission from different vibrational levels of the excited state. The emission spectra of **3-Gd**, excited at various wavelengths, is shown in Figure 4. The compound **3-Gd** in the solid state also exhibited intense green emission (Figure 5) when excited with UV light. Only one emission peak was observed at 533 nm by varying the excitation wavelength (354–390 nm) [52].

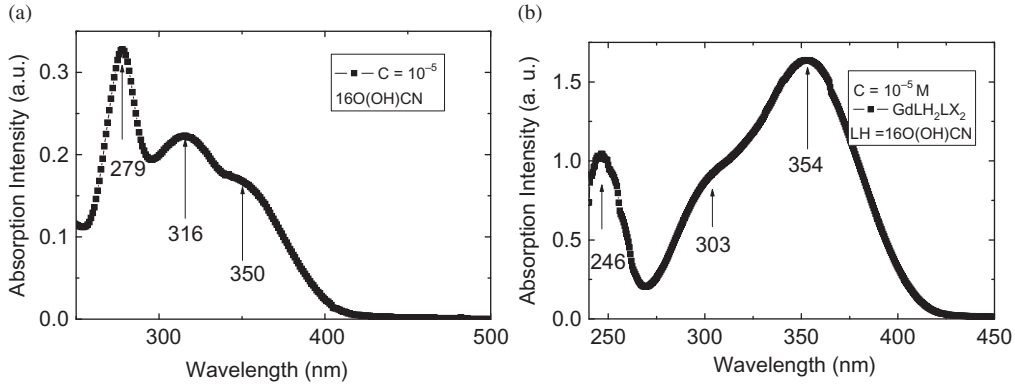

Figure 3. UV-Vis spectrum of (a) ligand **3** (10^{-5} M in chloroform) and (b) complex **3-Gd** (10^{-5} M Gd(III) complex in chloroform).

Table 2. Spectroscopic and photo-physical data in dichloromethane at room temperature.

Compound	λ max (nm) π–π* (ε, l mol^{-1} cm^{-1}))	Emission (nm) λ excitation	λ emission
1	242 (35,900), 288 (29,300), 341 (72,100) 421 (1600)	345	510
1-Cu	256 (102,600), 303 (152,000), 363 (79,500)		
1-VO	254 (215,600), 303 (151,100) 354 (141800)		
1-Gd	303 (45,000), 355 (58,000)	355	535
1-Pr	284 (81,800), 339 (163,500)	345	512
1-Sm	283 (41,300), 344 (45,500)	345	510
2	282 (134,700), 320 (94,800), 373 (114,000)	377	540
2-Cu	282 (44,100), 307 (33,600), 389 (9400)		
2-VO	281 (93,200), 314 (41,700)		
2-Gd	288 (18,100), 371 (56,700)	380	545
2-Sm	282 (45,300), 366 (89,800)	369	538
2-Pr	282 (38,700), 319 (25,300), 366 (22,400)	390	539
3	279 (32,800), 316 (22,300), 350 (16,800)	280	430
		340	430, 526
3-Cu	248 (26,400), 309 (41,600), 369 (23,800)		
3-VO	308 (43,200), 355 (49,500)		
3-Gd	246 (103,200),303 (90,800), 354 (163,700)	354	533
3-Pr	279 (56,400), 351 (45,500)	355	531
3-Sm	282 (68,400), 322 (59,400), 349 (57,900)	370	545

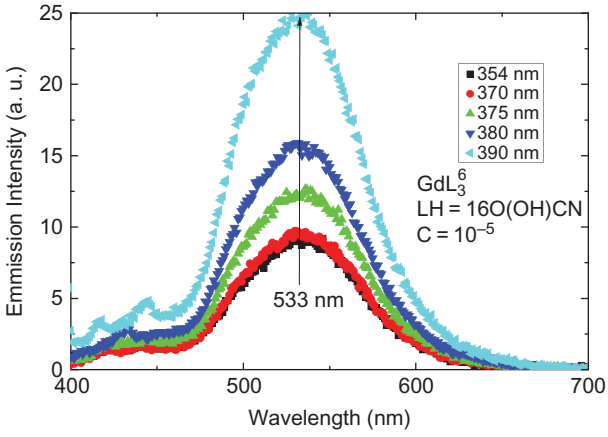

Figure 4. Fluorescence spectra of **3-Gd,** (Gd(III) complex of ligand **3** in chloroform at different excited wavelengths.

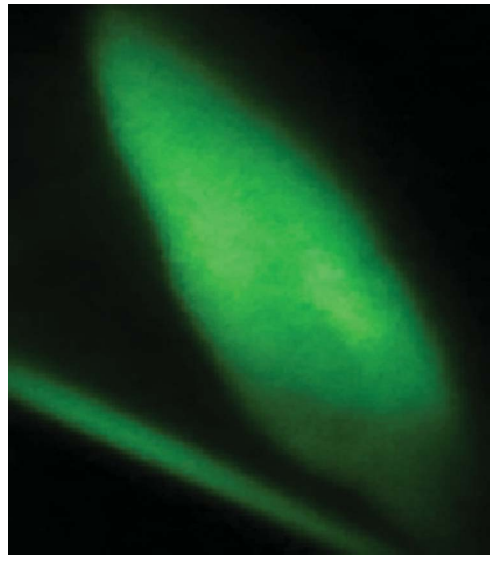

Figure 5. Fluorescent image of **3-Gd** in the solid state.

In lanthanide complexes the emission property of the corresponding ligand was retained because of steric hindrance in complexes due to the rigid molecular structure of the complex. The rigid molecular structure of the complexes restricts the free rotation and orientation of the emission dipole of the complex in the excited state [53]. This indicates the formation of a single conformer of the complex with a distinct electronic energy level. The UV-Vis and fluorescence spectra of **3-Sm** (Figure 6) and **3-Pr** also exhibited similar results. The absence of dual emission in methyl and nitro-substituted ligands (**1**, **2**) indicates that only one type of conformer is specifically formed.

5. Mesomorphism

5.1 Ligands

The mesogenic properties and phase transformations of all compounds were examined by a polarised optical microscope (POM) attached with a hot stage. The phase transition temperatures, along with the associated enthalpy and entropy changes, are investigated by DSC. The data is summarised in Table 3. The methyl-substituted ligand exhibited a monotropic nematic (N) phase, having four brush defects (Figure 7(a)), on cooling from the isotropic

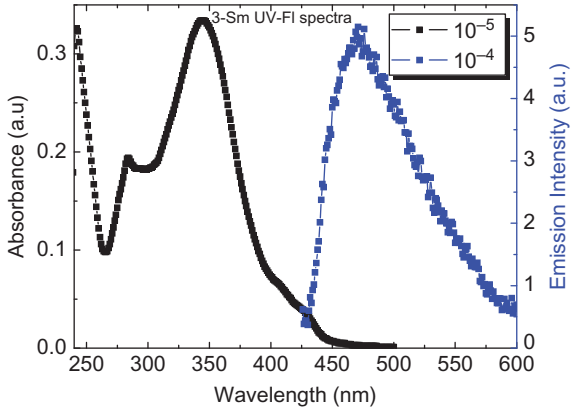

Figure 6. UV-Vis and fluorescence spectra of the Sm(III) complex, **3-Sm**, in chloroform.

phase at 70.5°C in the microscope, which appeared as a sharp peak in DSC at 70.4°C with a small enthalpy change of 2.74 kJ mol^{-1}. The nematic phase appeared over a very narrow temperature range of 1.6°C, which on further cooling crystallized to a solid phase at 68.9°C. This transition appeared as a broad peak in DSC at 68.9°C accompanied by a large enthalpy change (20.7 kJ mol^{-1}). Another peak appeared in DSC at a lower temperature due to a crystal-to-crystal transition at 67.4°C, which was not detected by microscopy. When the methyl group was replaced by cyano and nitro substituents, the clearing temperature of the compounds **2** and **3** increased along with the ordering of the mesophase. Both compounds (**2** and **3)** exhibited an enantiotropic SmA phase instead of a nematic (N) phase. The SmA phase of compounds **2** and **3** was recognised by characteristic battonets (a representative polarised optical microscopy texture of **3** is shown in Figure 7(b)) [54], arising from the dark isotropic phase on cooling, which were fully grown to a focal conic fan-like texture with some areas appearing black, indicating the homeotropic alignment of the molecules on lowering the temperature, and finally they were transformed to a crystalline phase. Both the transitions for **2** and **3** appeared as sharp peaks in the cooling cycle of DSC in the second heating and cooling cycle (the representative DSC spectrum of **3** is shown in Figure 7(c) at 127.5°C and 56.°C, with enthalpy changes of 7.08 and 69.3 kJ mol^{-1}, respectively, for compound **3**). It was observed that when the methyl group was replaced by polar groups, both the clearing temperatures to the isotropic phase and the width of the mesomorphic range increased. Nitro-substituted ligand **2** exhibited an enantiotropic SmA phase at a slightly elevated temperature compared with the cyano-substituted ligand **3**. This is because the presence of the polar group in the *para*-position of the aniline moiety, which increases the electronic polarisability along the long axis of the molecule and hence manifests liquid crystalline behaviour with an enhanced mesomorphic range of 65–72°C in comparison to the methyl-substituted compound (1.5°C).

In a previous report [55, 56] on lower homologues of similar compounds, viz. 7O(OH)X, where X = H, Me, NO_2 and CN, 7O(OH)H does not exhibit LC behaviour, while Me ($\Delta T \sim 14.0$°C, 12O(OH)Me: $\Delta T \sim 5.0$°C [25]) and cyano ($\Delta T \sim 41$°C) homologues exhibit only a nematic phase and nitro homologues ($\Delta T \sim 25.5$°C) exhibit nematic and SmA phases. A comparison of transition temperatures between the two homologous series (Table 4) revealed an increase in melting/crystallization temperatures with the increase in alkyl chain length. However, the width of the mesomorphic range (Table 4) decreases in compounds with methyl or methyloxy homologues when the alkyloxy chain of the salicylidene moiety changed from C7 to C16. In the case of polar end groups at one end of the molecule, the width of the mesomorphic range enormously increased in comparison to the methyl/oxy moiety. The increase in thermal ranges can be explained as follows. The thermal stability of the mesophase in these compounds is determined by the anisotropy of the contribution of the polarisability of X, the electronic structure of the N-phenyl moiety under the influence of the substituent inductive and resonance contributions and the associated change in the geometric anisotropy of the molecule. The contribution of substituent polarisability to the total polarisability and polarity of the molecule and the changes induced by the substituent X in the π-conjugation of the -CH=N-PhX fragment, as well as the conformation of the molecule, determine the thermal stability of the compounds. The methyl group in the N-phenyl moiety with stronger donor properties reduces the effect of π-conjugation of -CH=N-C_6H_4X, which is further augmented by the intramolecular H-bonding manifested between the proton of the ortho-hydroxyl group in the aldehyde moiety and the lone pair of the electrons on the nitrogen atom in the azomethine unit. Both of these effects contribute to increased planar conformation of the molecule in these compounds in comparison to the non-coplanarity of the phenyl rings on both sides of azomethine linkage in Schiff bases. Hence, the apparent stronger dispersion attraction between the planar molecules is reflected in the increase of melting temperature when H is replaced by the methyl group. The increased width of the mesomorphic range in nitro and cyano compounds is apparently due to distinct electronic properties, which contribute to strong intermolecular interactions with their additive contributions towards the total polarisability anisotropy of the molecules.

Table 3. Mesomorphic phase transition temperatures T^{0}C, associated enthalpies (ΔH kJ/mol) and entropies (ΔS J/K/mol) of the phase transitions of all ligand and complexes.

Abbreviation	Compound	Transition	T (^{0}C)	ΔH (kJmol^{-1})	ΔS (Jmol^{-1}K^{-1})	ΔT
1	16O(OH)1	K-I	84.6	53.8	150.5	–
	LH	I-N	70.4	2.74	7.9	–
		N-K	68.9	20.7	60.6	1.5[a]
		K-K1	67.4	1.0	2.9	–
1-Cu	$[16O(O)1]_2Cu$	K-I	119.5	47.4	–	–
	CuL_2	I-SmA	96.5	0.86	–	3.7[a]
		SmA-K	92.8	49.8	–	–
1-VO	$[16O(O)1]_2VO$	K-SmA	122.3	83.4	211.1	–
	VOL_2	SmA-I	128.1	5.03	12.5	5.8
		I-SmA	127.6	5.14	12.8	33.1
		SmA-K	94.5	38.2	104.0	
1-Gd[b]	$\{[Gd(16(OH)1)_2(16O(O)1)](NO_3)_2\}$	K-SmE	67.5	–	–	–
	$= \{[Gd(LH)_2(L)](NO_3)_2\}$	SmE-SmA	79.3	–	–	11.8
		SmA-I	152.5 dec	–	–	73.2
1-Pr	$\{[Pr(16(OH)1)_2(16O(O)1)](NO_3)_2\}$	K-SmE	56.4	15.5	47.1	100.3
	$= \{[Pr(LH)_2(L)](NO_3)_2\}$	SmE-SmA	84.2	7.9	22.1	Heating
		SmA-I	156.7 dec	6.2	14.5	cycle
1-Sm[b]	$\{[Sm(16(OH)1)_2(16O(O)1)](NO_3)_2\}$	K-SmA	82.3			–
	$= \{[Sm(LH)_2(L)](NO_3)_2\}$	SmA-I	159.2 dec			76.9
2	$16O(OH)NO_2$	K-SmA	79.7	46.3	131.4	–
	LH	SmA-I	130.8	3.91	9.68	51.1
		I-SmA	130.0	3.96	9.82	64.9
		SmA-K	65.1	38.9	115.2	–
2-Cu	$[16O(O)NO_2]_2Cu$	K-K1	132.3	6.07	14.9	–
	CuL_2	K1-I	144.7	8.33	19.9	–
		I-SmA	131.4	3.41	8.45	–
		SmA-SmE	105.1	17.9	47.4	26.3[a]
		SmE-K	90.2	12.1	33.5	14.9
2-VO	$[16O(O)NO_2]_2VO$	K-SmA	103.7	6.26	16.6	–
	VOL_2	SmA-I	167.5	3.85	8.74	63.8
		I-SmA	165.1	4.21	10.8	66.3
		SmA-K	98.8	5.35	14.4	–
2-Gd[b]	$\{[Gd(16(OH)NO_2)_2(16O(O)NO_2)](NO_3)_2\}$	K-SmA	71.6	–	–	96.9
	$= \{[Gd(LH)_2(L)](NO_3)_2\}$	SmA-I	168.5 dec	–	–	–
2-Pr[b]	$\{[Pr(16(OH)NO_2)_2(16O(O)\ NO_2)](NO_3)_2\}$	K-SmA	106.5	–		74.1
	$= \{[Pr(LH)_2(L)](NO_3)_2\}$	SmA-I	180.6 dec	–		–
2-Sm[b]	$\{[Sm(16(OH)NO_2)_2(16O(O)NO_2)](NO_3)_2\}$	K-SmA	111.5	–	–	56.3
	$= \{[Sm(LH)_2(L)](NO_3)_2\}$	SmA-I	167.8 dec	–	–	–
3	16O(OH)CN	K-SmA	72.9	70.2	202.9	–
	LH	SmA-I	128.7	8.38	20.8	55.8
		I-SmA	127.5	7.08	17.6	71.2
		SmA-K	56.3	69.3	210.5	–
3-Cu	$[16O(O)CN]_2Cu$	K-SmA	115.9	33.0	84.9	–
	CuL_2	SmA-I	146.3	4.10	9.7	30.4
		I-SmA	145.6	4.93	11.7	53.6
		SmA-K	92.0	6.40	17.5	–
3-VO	$[16O(O)CN]_2VO$	K-I	151.1	10.1	23.8	–
	VOL_2	I-SmA	137.6	1.50	3.66	–
		SmA-K	118.3	10.3	26.4	19.3[a]
3-Gd[b]	$\{[Gd(16O(OH)CN)_2(16O(O)CN)](NO_3)_2\}$	K-SmX1	54.8	–	–	110.4
	$= \{[Gd(LH)_2(L)](NO_3)_2\}$	SmX1-I	165.2 dec	–	–	–
3-Pr[b]	$\{[Pr(16O(OH)CN)_2(16O(O)CN)](NO_3)_2\}$	K-SmA	74.8	–	–	82.4
	$= \{[Pr(LH)_2(L)](NO_3)_2\}$	SmA-I	157.2 dec	–	–	–
3-Sm[b]	$\{[Sm(16O(OH)CN)_2(16O(O)CN)](NO_3)_2\}$	K-SmA	84.5	–	–	64.8
	$= \{[Sm(LH)_2(L)](NO_3)_2\}$	SmA-I	149.3 dec	–	–	–

[a]Monotropic transition., [b]observed by POM studies. LH =16O(OH)X, **1 = LH;** X = CH_3, **2 = LH; X** = NO_2, **3 = LH; X** = CN, dec = decomposes

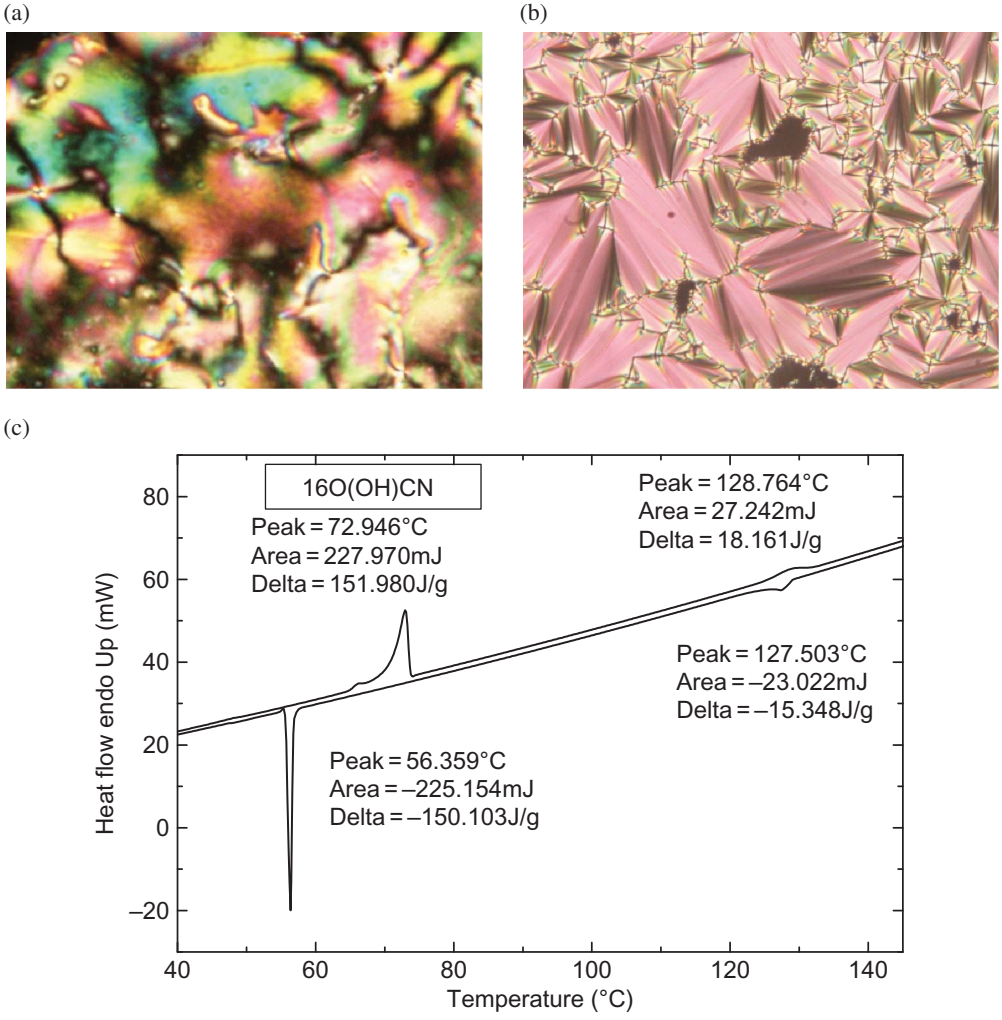

Figure 7. (a) Schlieren texture of the nematic phase exhibited by **1** at 70.2°C. (b) Focal conic fan texture of the SmA phase exhibited by **3** at 58°C. (c) Differential scanning calorimetry spectrum of compound **3** in the second heating and cooling cycles at 5°C min^{-1}.

Table 4. Comparison of transition temperatures in °C and the mesomorphic range of ligands and complexes in °C.

		H	OMe	Me	F	Cl	NO_2	CN	Ref
Melting point/ crystallisation of 16O(OH)X	Heating	79.4	100.5	84.6	83.6	87.9	79.7	72.9	Present work, 36
	Cooling	67.2	86.3	68.9	72.6	71.9	65.1	56.3	
Melting point of 7O(OH)X	Heating	50.9	90.0	64.9	73.0	72.0	76.0	80.0	51
Δ*T* of 16O(OH)X		0.1	15.0	1.5	2.3	34.0	64.9	71.2	36
Δ*T* of 7O(OH)X		0.0	16.9	14.0	(0.5)	50.0	25.5	41.0	51
Δ*T* [16O(O)X]$_2$Cu		0.0	60.2	3.7	30.1	67.6	41.0	53.6	36
Δ*T* [7O(O)X]$_2$Cu		0.0	7.1	0.0	20.4	31.2	0.0	0.0	52
Δ*T* [16O(O)X]$_2$VO			136.0	33.1	103.3	92.6	66.3	19.3	36
12O(OH)1: K 78 N 83 I; Cu[12O(O)1]$_2$:K 126 I; VO[12O(O)1]$_2$:K 135 I									25

5.2 Complexes

All the complexes were synthesised following the standard literature procedures, and in some cases procedures were modified depending on the condition of precipitation of the complexes. It was observed that complexes derived from *f*-block metal ions were highly viscous and exhibited higher clearing (mesomorphic–isotropic) transition temperatures than their corresponding *d*-block metal analogues. This is because of basic differences in the molecular structure

of the complexes. The *d*-block metal can coordinate with two Schiff bases, which provides four coordination sites resulting in square planar (Cu(II) complex) and square pyramidal (VO(IV) complex) structures. The lanthanide ion (*f*-block metal) has a higher coordination number than that of transition metal ions, and hence it can coordinate with three or more Schiff bases, which increase the thermal stability of these complexes.

1-Cu, the Cu(II) complex of methyl-substituted ligand, exhibited a monotropic SmA phase (Figure 8(a)) on cooling (~3°C) whereas **1-VO**, the vanadium analogue, exhibited an enantiotropic SmA phase (Figure 8(b)), with an enhanced mesomorphic thermal range (~33°C). The presence of an oxygen atom in the apical position of vanadium complexes increases the intermolecular interaction, which stabilises the layer formation and hence increases the mesomorphic range. In the complexes derived from polar ligands [**2-Cu**, **2-VO** and **3-Cu**], it was observed that both the mesomorphic–isotropic temperature and the width of the mesomorphic range of the SmA phase have been enhanced (41–60°C), except **3-VO** (only monotropic SmA phase), compared to methyl-substituted complexes. Nitro-substituted copper complex **2-Cu** exhibited a higher order smectic E (SmE) phase below the SmA phase, which was identified by the appearance of arcs across the focal conic fans (the representative polarised optical microscopy texture of **2-Cu** is shown in Figure 9(a)) observed in the SmA phase on lowering the temperature. The SmE phase is also confirmed by POM studies in a contact preparation with a standard sample reported earlier [17]. **2-VO** of the nitro-substituted ligand exhibited only the SmA phase. Cyano-substituted complexes exhibited typical focal conic fan textures characteristic of the SmA phase for both **3-Cu** (the representative DSC spectrum of **3-Cu** is shown in Figure 9(c)) and **3-VO** (the polarised optical microscopy texture as shown in Figure 9(b)) on cooling. In these *d*-block complexes the thermal stability of vanadium complexes is much higher, as evidenced by higher melting and clearing temperatures due to stronger intermolecular and interlayer interactions, due to the presence of an apical oxygen atom.

Upon going from the ligands to the complexes, the length as well as width of the molecule sharply increases, thereby enhancing dispersion interactions. These interactions increase the anisotropy of the intermolecular dispersion interactions to widen the mesomorphic range in the complexes in comparison to ligands. A comparison of mesomorphic range in copper complexes when alkyloxy chain increased from C7 to C16, revealing substantial increase in the width of the mesomorphic range (Table 2). Even though the increase in molecular width of copper complexes is the same in C7 and C16 homologues, the increased length of the molecules enhanced the geometric anisotropy of the complexes and hence increased the anisotropy of the intermolecular dispersion interactions to enhance the mesomorphic range.

Among the lanthanide complexes of methyl-substituted ligand, both Gadolinium (**1-Gd**) and Praseodymium (**1-Pr**) complexes exhibit optical textures characteristic of SmE (Figure 10(a)) and SmA (Figure 10(b)) phases, but in DSC the complex (the representative DSC spectrum of **1-Pr** is shown in Figure 10(c)) decomposed on heating above the clearing temperature. **1-Sm** exhibits only the SmA phase in both heating and cooling. The lanthanide complexes (**2-Gd**, **2-Sm**, **2-Pr**, **3-Gd, 3-Sm** and **3-Pr**) derived from polar ligands (**2** and **3**) are highly viscous in nature. **2-Gd** and **2-Sm** complexes exhibited an enantiotropic SmA phase with a focal conic fan texture, whereas **2-Pr** exhibited a SmA phase only in heating and decomposed above clearing temperature. Cyano-substituted lanthanide complexes, viz. **3-Pr** and **3-Sm** (the focal conic fan texture of the SmA phase is shown in Figure 11), exhibited an enantiotropic SmA phase. **3-Gd** exhibited an unspecified texture and further work is in progress for the phase identification. We could not observe well-defined transition peaks in

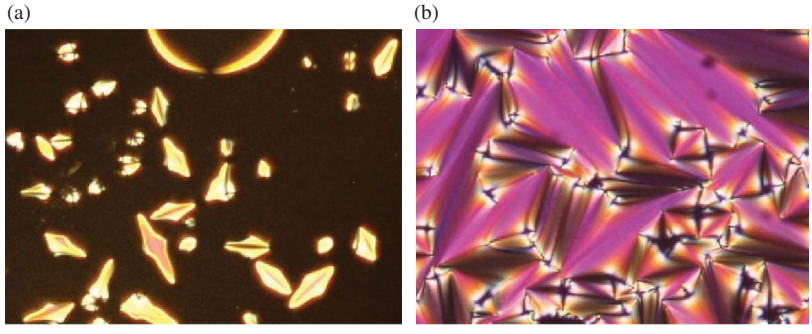

Figure 8. (a) **1-**battonets and homeotropic texture of the SmA phase exhibited by **1-Cu** at 95.4°C. (b) **1-**focal conic fan texture of the SmA phase exhibited by **1-VO** at 125.8°C.

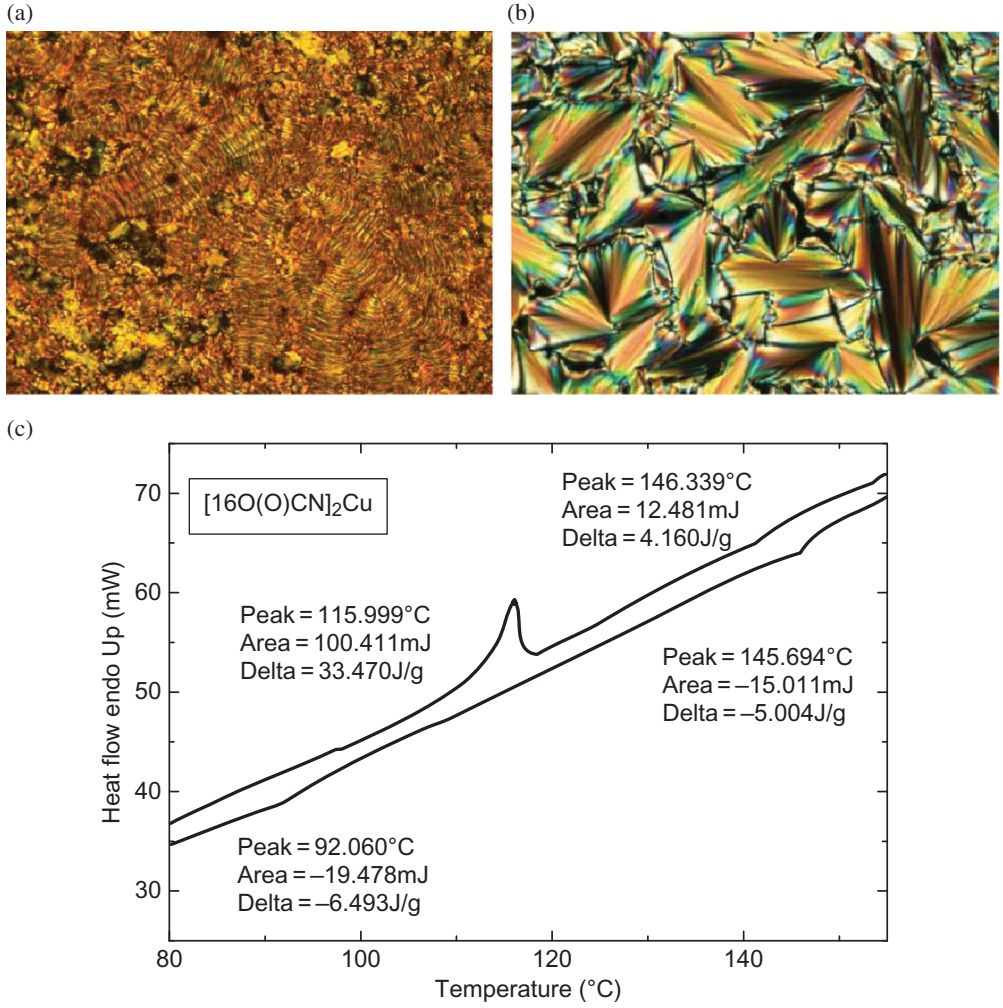

Figure 9. (a) Focal conic fan texture with arcs across the fans of the SmE phase exhibited by **2-Cu** at 102°C. (b) Focal conic fan texture of the SmA phase exhibited by **3-VO** at 133.5°C. (c) Differential scanning calorimetry spectrum of compound **3-Cu** in the second heating and cooling cycles at 5°C min^{-1}.

DSC of these lanthanide complexes due to their high viscous nature. Hence, only the observed transition temperatures under polarised optical microscopy are reported for lanthanide complexes in Table 3. An increase in polarity increases both van der Waals and ionic interactions between the molecules, which contribute to the decrease in interlayer distance and increase in viscosity, as well as to the melting and clearing temperatures of the complexes. Furthermore, some of these complexes decomposed in the vicinity of the mesomorphic–isotropic transition temperature, unlike the complexes with an alkyl moiety in the ligand [39].

6. Conclusions

Three Schiff base ligands with methyl (**1**) nitro (**2**) and cyano (**3**) substituents and their corresponding copper, vanadium and lanthanide complexes (Gd(III), Sm(III) and Pr(III)) of the ligands with a polar substituent at one end of the molecule have been successfully synthesised and their photo-physical and mesomorphic properties were studied. All the ligands exhibited fluorescence when excited at ~345 nm. Cyano-substituted ligand **3** exhibited dual fluorescence when excited at 300–340 nm due to the formation of different conformers with association of the solvent molecule. The importance of a long alkyl chain length at one end, promoting increased dispersion anisotropy, and a polar moiety at the other end of the molecule to augment strong intermolecular interactions in salicylideneimine derivatives exhibiting a wide mesomorphic range and higher thermal stability, has been described. It is found that the manifestation of mesomorphism in ligands, as well as their complexes, is influenced by the polar end group and long alkyl chain length. Hence, competing influences between the alkyl chain

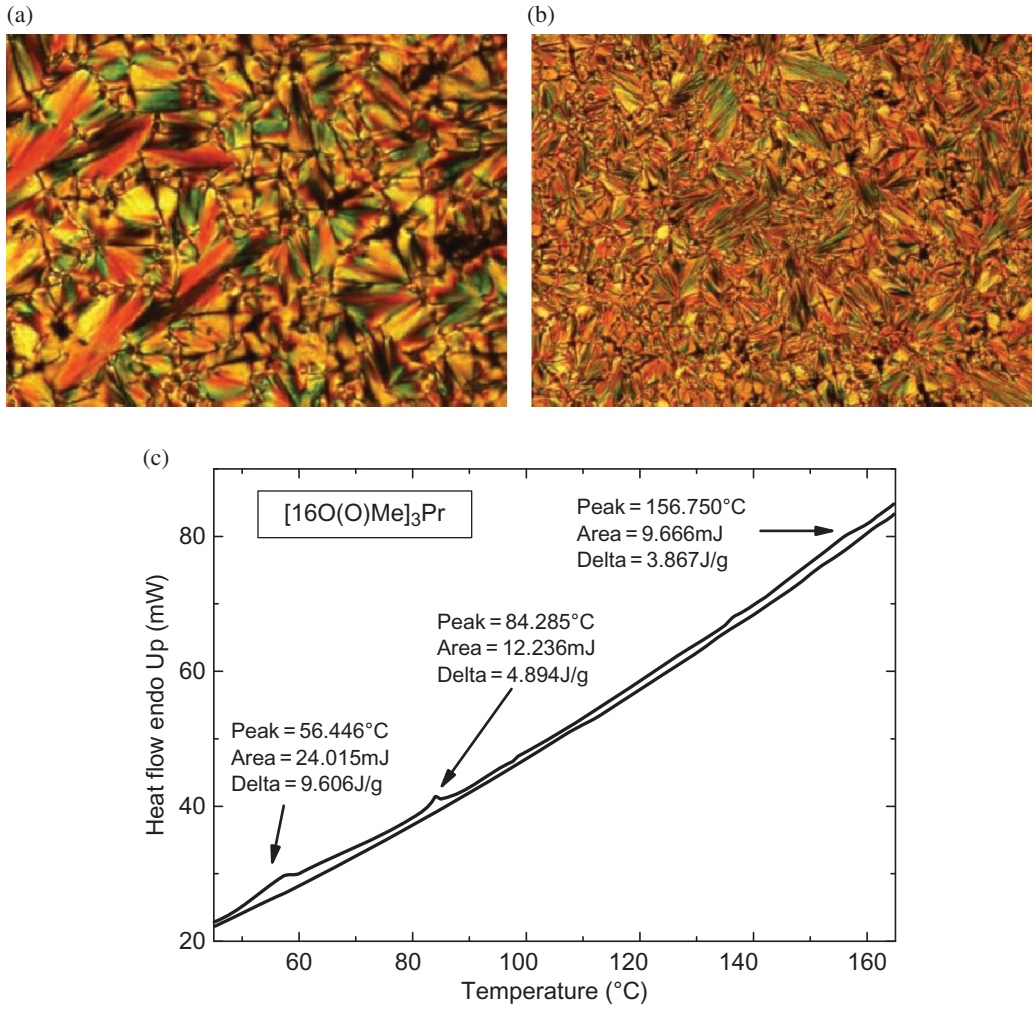

Figure 10. (a) Focal conic fan texture of the SmA phase exhibited by **1-Pr** at 154.1°C. (b) Optical texture super cooled to room temperature **1-Pr,** at 30°C. (c) Differential scanning calorimetry spectrum of compound **1-Pr** in the first heating and cooling cycles at 5°C min^{-1}.

length and electronic nature of the substituent plays an important role in the mesomorphism of these complexes. The nematic phase was only observed in the methyl-substituted ligand, whereas the SmA phase was predominantly observed for all others.

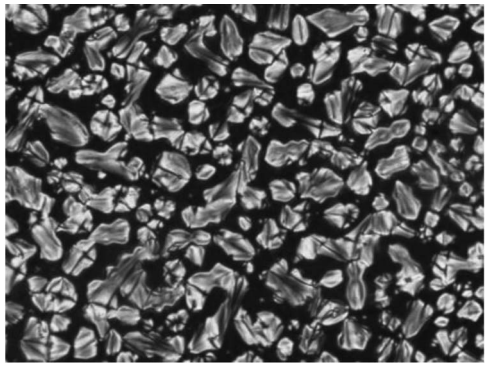

Figure 11. Focal conic fan texture of the SmA phase exhibited by **3-Sm** at 138.5°C.

In particular, the special experimental challenge of synthesis of lanthanide-containing LCs, viz. salicylideneimine-based promesogenic ligands, with *a polar group substituted in an aryl moiety on a nitrogen atom of the central bridging imine group* is fulfilled. The lanthanide complexes exhibit a large thermotropic mesomorphic range (56–110°C), exhibiting SmA and SmE phases. Lanthanide complexes exhibited higher clearing temperatures than the transition metal complexes. The major advantage of lanthanide-containing metallomesogens is intense luminescence characteristics at a single wavelength when excited either at lower or higher wavelengths. The magnetic anisotropy and X-ray investigations of these complexes are still to be explored and further work is in progress to synthesise stable room temperature

lanthanidomesogens exhibiting nematic and smectic phases by suitable changes in the end alkyl chains, substituents in the aromatic core and counter-ions.

7. Preparation of ligands and metal complexes

7.1 Synthesis of aldehyde

4-*n*-hexadecyloxy salicylaldehyde was synthesised as described earlier [17, 57–59] using the modified Williamson's method. A total of 1 mmol of 1-bromohexadecane and 1 mmol of 4-hydroxysalicylaldehyde was heated under reflux in the presence of $KHCO_3$ (1 mmol) as a base in dry acetone. The product was purified by column chromatography using hexane as the eluent.

7.2 Synthesis of the Schiff bases

The free ligands were synthesised following a well-known procedure [57–59] by refluxing a mixture of ethanolic solution of 1 mmol of the 4-*n*-hexadecyloxysalicylaldehyde with 1 mmol of appropriate amine and few drops of glacial acetic acid as a catalyst for four hours. The precipitated product was purified by repeated recrystallisation from absolute ethanol until constant clearing temperatures were achieved (yield 65–70%).

1: N-(4-*n*-hexadecyloxysalicylidene)-4′-methylaniline, 16O(OH)CH_3

Yield: 75%, IR (KBr) $\nu = 1627\ cm^{-1}$ (stretching C=N), ^1H NMR (400 MHz, $CDCl_3$), $\delta = 13.93$ (s, 1H, -OH-), 8.58 (s, 1H, -CH=N-), 7.23 (d, 2H, 8.4), 7.29 (d, 1H, 8.8), 6.48 (d, 2H, 8.8), 7.16 (d, 2H), 4.01 (t, 2H, 6.8), 2.42 (s, 3H, CH_3 of aniline ring), 1.85–1.77 (q, 2H, 6.8), 1.51–1.44 (m, 26H), 0.91 (t, 3H, 7.6) ppm. $C_{30}H_{45}NO_2$ (451.68); elemental analysis: calculated, C, 79.77; H, 10.04; N, 3.10; found C, 79.19; H, 9.99; N, 3.09%.

2: N-(4-*n*-hexadecyloxysalicylidene)-4′- nitroaniline, 16O(OH)NO_2

Yield: 65%, IR (KBr) $\nu = 1627\ cm^{-1}$ (stretching C=N), ^1H NMR (500 MHz, $CDCl_3$), $\delta = 13.07$ (s, 1H, -OH-), 8.54 (s, 1H, -CH=N-),7.31 (d, 2H), 7.33(d, 1H, 8.9), 6.52 (d, 2H, $J = 8.6$), 8.29 (d, 2H, $J = 6.8$), 4.01 (t, 2H, 6.6), 1.82–1.78 (q, 2H), 1.60–1.26 (m, 26H), 0.89 (t, 3H, 6.9) ppm. $C_{29}H_{42}N_2O_4$ (482.65); elemental analysis: calculated, C, 72.17; H, 8.77; N, 5.80; found C, 71.99; H, 8.73; N, 5.53%.

3: N-(4-n-hexadecyloxysalicylidene)-4′- cyanoaniline, 16O(OH)CN

Yield: 65%, IR (KBr) $\nu = 2222\ cm^{-1}$ (stretching C≡N), $1627\ cm^{-1}$ (stretching C=N), ^1H NMR (500 MHz, $CDCl_3$), δ: 13.13(s, 1H, -OH-), 8.51 (s, 1H, -CH=N-), 7.28–7.26 (d, 2H, 7.6), 7.30 (d, 1H, 9.2 Hz), 6.51(d, 2H), 7.69 (d, 2H, 8.4), 4.00 (t, 2H, 6.1), 1.79 (q, 2H, 6.6), 1.5–1.25 (m, 26H), 0.89 (t, 3H, 6.8) ppm. $C_{30}H_{42}N_2O_2$ (462.67); elemental analysis: calculated, C, 77.88; H, 9.15; N, 6.05; found C, 77.25; H, 9.01; N, 5.89%.

7.3 Preparation of the metal complexes

The synthesis of copper(II) complexes was carried out by refluxing the mixture consisting of slowly added ethanolic copper(II) acetate [$Cu(OAc)_2.H_2O$] (1 mmol) solution (20 ml) to a hot solution of the appropriate ethanolic imine (2 mmol) solution (∼50 ml) for four hours. The solution was cooled to room temperature and filtered to yield the brown copper (II) complexes, which were subsequently recrystallised from a mixture of ethyl acetate and ethanol.

1-Cu: Yield: 62%, IR (KBr) $\nu = 1616\ cm^{-1}$ (stretching C=N), $C_{60}H_{88}CuN_2O_4$ (964.90); elemental analysis: calculated, C, 74.69; H, 9.19; N, 2.90; found C, 74.55; H, 9.06; N, 2.67%.

2-Cu: Yield: 70%, IR (KBr) $\nu = 1608\ cm^{-1}$ (stretching C=N), $C_{58}H_{82}CuN_4O_8$ (1026.84); elemental analysis: calculated, C, 67.84; H, 8.05; N, 5.46; found C, 67.24; H, 8.00; N, 5.16%.

3-Cu: Yield: 55%, IR (KBr) $\nu = 1612\ cm^{-1}$ (stretching C=N), $2222\ cm^{-1}$ (stretching C≡N), $C_{60}H_{82}CuN_4O_4$ (986.86); elemental analysis: calculated, C, 73.02; H, 8.38; N, 5.68; found C, 72.89; H, 8.29; N, 5.15%.

Oxovanadium (1V) complexes were prepared by refluxing the mixture consisting of slowly added 20 ml of vanadium(1V) oxide sulphate ($VOSO_4.5H_2O$) (1 mmol) solution in methanol to a hot solution of the appropriate imine (2 mmol) in methanol (50 ml) in the presence of triethylamine for four hours. The solution was cooled to room temperature and filtered to yield the green oxovanadium (1V) complexes, which were subsequently recrystallised from a mixture of ethyl acetate and ethanol.

1-VO: Yield: 45%, IR (KBr) ν = 1608 (stretching C=N), 987 cm^{-1} (stretching V=O), $C_{60}H_{88}N_2O_5V$ (968.29); elemental analysis: calculated C, 74.42; H, 9.16; N, 2.89; found C, 74.11; H, 9.01; N, 2.65%.

2-VO: Yield: 55%, IR (KBr) ν = 1608 (stretching C=N), 970 cm^{-1} (stretching V=O), $C_{58}H_{82}N_4O_9V$, (1030.23); elemental analysis: calculated C, 67.62; H, 8.02; N, 5.44; found C, 67.11; H, 8.05; N, 5.13%.

3-VO: Yield: 45%, IR (KBr) ν = 2222, (stretching C≡N), 1610 cm^{-1} (stretching C=N), 966 cm^{-1} (stretching V=O), $C_{60}H_{82}N_2O_5V$ (990.26); elemental analysis: calculated C, 72.77; H, 8.35; N, 5.66; found C, 72.15; H, 8.25; N, 5.15%.

For gadolinium (III) complexes, the mixture containing gadolinium (III) nitrate [$Gd(NO_3)_3$] (1 mmol) solution in acetonitrile (20 ml) and a hot solution of the appropriate imine (3 mmol) solution in acetonitrile (~50 ml) was heated under reflux for four hours to yield the desired product. The solution was filtered when it was hot to avoid the impurity of unreacted ligand and to yield the pale yellow precipitate of gadolinium (III) complexes, which were washed repeatedly with acetonitrile. The precipitate was dried for further analysis.

1-Gd: Yield: 45%, IR (KBr) ν = 1639, 1602 cm^{-1}, $C_{90}H_{134}GdN_5O_{12}$ (1635.30); elemental analysis: calculated C, 66.10; H, 8.26; N, 4.28; found C, 65.91; H, 8.14; N, 4.11%.

2-Gd: Yield: 35%, IR (KBr) ν = 1639, 1602 cm^{-1}, $C_{87}H_{125}GdN_8O_{18}$ (1728.22); elemental analysis: calculated C, 60.46; H, 7.29; N, 6.48; found C, 60.11; H, 7.21; N, 6.11%.

3-Gd: Yield: 35%, IR (KBr) ν = 1639, 1602 cm^{-1}, $C_{90}H_{125}GdN_8O_{12}$ (1668.25); elemental analysis: calculated C, 64.80; H, 7.55; N, 6.72; found C, 64.12; H, 7.65; N, 6.17%.

For praseodymium (III) complexes, the mixture containing praseodymium (III) nitrate [$Pr(NO_3)_3$] (1 mmol) solution in acetonitrile (20 ml) and a hot solution of the appropriate imine (3 mmol) solution in acetonitrile (~50 ml) was heated under reflux for four hours to yield the desired product. The solution was filtered when it was hot to avoid the impurity of unreacted ligand and to yield the pale yellow precipitate of praseodymium (III) complexes, which were washed repeatedly with acetonitrile. The precipitate was dried for further analysis.

1-Pr: Yield: 31%, IR (KBr) ν = 1639, 1602 cm^{-1}, $C_{90}H_{134}N_5O_{12}Pr$ (1618.96); elemental analysis: calculated C, 66.77; H, 8.34; N, 4.33; found C, 65.69; H, 8.03; N, 4.09%.

2-Pr: Yield: 37%, IR (KBr) ν = 1641, 1602 cm^{-1}, $C_{87}H_{125}N_8O_{18}Pr$ (1711.8); elemental analysis: calculated C, 61.04; H, 7.36; N, 6.55; found C, 60.71; H, 7.28; N, 6.18%.

3-Pr: Yield: 28%, IR (KBr) ν = 1642, 1602 cm^{-1}, $C_{90}H_{125}N_8O_{12}Pr$ (1651.91); elemental analysis: calculated C, 65.44; H, 7.63; N, 6.78; found C, 65.14; H, 7.33; N, 6.25%.

For samarium (III) complexes, the mixture containing samarium (III) nitrate [$Sm(NO_3)_3$] (1 mmol) solution in acetonitrile (20 ml) and a hot solution of the appropriate imine (3 mmol) solution in acetonitrile (~50 ml) was heated under reflux for four hours to yield the desired product. The solution was filtered when it was hot to avoid the impurity of unreacted ligand and to yield the pale yellow precipitate of samarium (III) complexes, which were washed repeatedly with acetonitrile. The precipitate was dried for further analysis.

1-Sm: Yield: 31%, IR (KBr) ν = 1639, 1602 cm^{-1}, $C_{90}H_{134}N_5O_{12}Sm$ (1628.41); elemental analysis: calculated C, 66.38; H, 8.29; N, 4.30; found C, 66.09; H, 8.13; N, 4.07%.

2-Sm: Yield: 25%, IR (KBr) ν = 1643, 1602 cm^{-1}, $C_{87}H_{125}N_8O_{18}Sm$ (1721.33); elemental analysis: calculated C, 60.70; H, 7.32; N, 6.51; found C, 60.23; H, 7.15; N, 5.87%.

3-Sm: Yield: 26%, IR (KBr) ν = 1639, 1602 cm^{-1}, $C_{90}H_{125}N_8O_{12}Sm$ (1661.36); elemental analysis: calculated C, 65.06; H, 7.58; N, 6.74; found C, 64.31; H, 7.35; N, 6.23%.

Acknowledgements

The authors acknowledge the financial assistance from Department of atomic energy, department of science and technology and university grants commission.

References

[1] Serrano, J.L., Ed. *Metallomesogens, Synthesis, Properties and Applications*; VCH: Weinheim, Germany, 1996.
[2] Giroud-Godquin, A.M. Metal-containing liquid crystals. In *Handbook of Liquid Crystals*: Demus, D.; Goodby, J.; Gray, G.W.; Spiess, H.W.; Vill, V., Eds.; Wiley-VCH: Weinheim, Germany, 1998; Vol. IIB, pp 901–932.
[3] Giroud-Godquin, A.M.; Maitlis P.M. *Angew. Chem. Int. Ed. Engl*. **1991**, *30*, 375–402.
[4] Espinet, P.; Esteruelas, M.A.; Oro, L.A.; Serrano, J.L.; Sola, E. *Coord. Chem. Rev*. **1992**, *117*, 215–274.
[5] Bruce, D.W. *Inorganic Materials*, 2nd ed.: Bruce, D.W.; O'Hare, D. Eds.; Wiley: Chichester, 1996; Ch. 8, pp 405–490.
[6] Bruce, D.W. *J. Chem. Soc. Dalton Trans*. **1993**, 2983–2989.
[7] Polishchuk, A.P.; Timofeeva, T.V. *Russ. Chem. Rev*. **1993**, *62*, 291–321.
[8] Hudson, S.A.; Maitlis, P.M. *Chem. Rev*. **1993**, *93*, 861–865.
[9] Oriol, L.; Serrano, J.L. *Adv. Mater. (Weinheim, Ger.)* **1995**, *7*, 348–369.
[10] Hoshino, N. *Coord. Chem. Rev*. **1998**, *174*, 77–108.
[11] Donnio, B.; Bruce, D.W. *Struct. Bond*. **1999**, *95*, 193–247.
[12] Donnio, B.; Guillon, D.; Deschenaux, R.; Bruce, D.W. *Comprehensive Coordination Chemistry II: From Biology to Nanotechnology*: McCleverty, J.A.; Meyer, T.J., Eds.; Elsevier: Oxford, 2003; Vol. 7, pp 357–627.
[13] Bruce, D.W.; Deschenaux, R.; Donnio, B.; Guillon, D. *Comprehensive Organometallic Chemistry III*: Crabtree, R.H.; Mingos, D.M.P., Eds.; Elsevier: Oxford, 2007; Vol. 12. Ch. 12.05, pp 195–293.

[14] Galyametdinov, Y.G.; Ivanova, G.I.; Ovchinnikov, I.V. *Izv. Akad. Nauk. SSSR, Ser. Khim*. **1989**, *5*, 1232.
[15] Rao, N.V.S.; Singha, D.; Das, M.; Paul, M.K. *Mol. Cryst. Liq. Cryst*. **2002**, *373*, 106–117.
[16] Martin, F.; Collinson, S.R.; Bruce, D. *Liq. Cryst*. **2000**, *27*, 859–863.
[17] Rao, N.V.S.; Choudhury, T.D.; Paul, M.K.; Francis, T. *Liq. Cryst*. **2009**, *36*, 409–423.
[18] Ghedini, M.; Pucci, D.; Munno, G.D.; Viterbo, D.; Neve, F.; Armentano, S. *Chem. Mater*. **1991**, *3*, 65–72.
[19] Ghedini, M.; Longeri, M.; Bartolino, R. *Mol. Cryst. Liq. Cryst*. **1982**, *84*, 207–211.
[20] Ghedini, M.; Licoccia, S.; Armentano, S.; Bartolino, R. *Mol. Cryst. Liq. Cryst*. **1984**, *108*, 269–275.
[21] Ghedini, M.; Morrone, S.; Bartolino, R.; Formoso, V.; Francescangeli, O.; Yang, B.; Gatteschi, D.; Znachini, C. *Chem. Mater*. **1993**, *5*, 876–882.
[22] Ghedini, M.; Morrone, S.; Francescangeli, O.; Bartolino, R. *Chem. Mater*. **1994**, *6*, 1971–1977, and *ibid*. **1992**, *4*, 1119–1123.
[23] Paschke, R.; Liebsch, S.; Tschierske, C.; Oakley, M.A.; Sinn, E. *Inorg. Chem*. **2003**, *42*, 8230–8240.
[24] Marcos, M.; Romero, P.; Serrano, J.L.; Bueno, C.; Cabeza, J.A.; Oro, L.A. *Mol. Cryst. Liq. Cryst*. **1989**, *167*, 123–134.
[25] Ghedini, M.; Morrone, S.; Gatteschi, D.; Zanchini, C. *Chem. Mater*. **1991**, *3*, 752–758.
[26] Bhattacharjee, C.R.; Das, G.; Mondal, P.; Prasad, S.K.; Rao, D.S.S. *Liq. Cryst*. **2011**, *38*, 615–623.
[27] Bhattacharjee, C.R.; Das, G.; Purkayastha, D.D.; Mondal, P. *Liq. Cryst*. **2011**, *38*, 717–727.
[28] Binnemans, K. *Mat. Sci. Forum* **1999**, *315*, 169–174.
[29] Galyametdinov, Yu.G.; Athanassopoulou, M.A.; Griesar, K.; Kharitonova, O.; Soto Bustamante, E.A.; Tinchurina, L.; Ovchinnikov, I.; Haase, W. *Chem. Mater*. **1996**, *8*, 922–926.
[30] Binnemans, K.; Gorller-Walrand, C. *Chem. Rev*. **2002**, *102*, 2303–2345.
[31] Binnemans, K.; Galyametdinov, Yu.G.; Van Deun, R.; Bruce, D.W.; Collinson, S.R.; Polishchuk, A.P.; Bikchantaev, I.; Haase, W.; Prosvirin, A.V.; Tinchurina, L.; Litvinov, I.; Gubajdullin, A.; Rakhmatullin, A.; Uytterhoeven, K.; Van Meervelt, L. *J. Am. Chem. Soc*. **2000**, *122*, 4335–4344 and references therein.
[32] Binnemans, K.; Bruce, D.W.; Collinson, S.R.; Van Deun, R.; Galyametdinov, Yu.G.; Martin, F. *Phil. Trans. R. Soc. Lond. A* **1999**, *357*, 3063–3077.
[33] Galyametdinov, Y.G.; Haase, W.; Malykhina, L.; Prosvirin, A.; Bikchantaev, I.; Rakhmatullin, A.; Binnemans, K. *Chem. Eur. J*. **2001**, *7*, 99–105.
[34] Van Deun, R.; Binnemans, K. *J. Alloy. Comp*. **2000**, *303–304*, 146–150.
[35] Bellusci, A.; Barberio, G.; Crispini, A.; Ghedini, M.; La Deda, M.; Pucci, D. *Inorg. Chem*. **2005**, *44*, 1818–1825.
[36] Cardinaels, T.; Driesen, K.; Parac-Vogt, I.N.; Heinrich, B.; Bourgogne, C.; Guillon, D.; Donnio, B.; Binnemans, K. *Chem. Mater*. **2005**, *17*, 6589–6598.
[37] Mukai, H.; Yokokawa, M.; Hatsusaka, K.; Ohta, K. *Liq. Cryst*. **2010**, *37*, 13–21.
[38] Rao, N.V.S.; Paul, M.K.; Rao, T.R.; Prasad, A. *Liq. Cryst*. **2002**, *29*, 1243–1246.
[39] Rao, N.V.S.; Choudhury, T.D.; Deb, R.; Paul, M.K.; Rao, T.R.; Francis, T.; Smalyukh, I.I. *Liq. Cryst*. **2010**, *37*, 1393–1410.
[40] Chakraborty, L.; Chakraborty, N.; Laskar, A.R.; Paul, M.K.; Rao, N.V.S. *J. Mol. Struct*. **2011**, *1002*, 135–144.
[41] Collinson, S.R.; Martin, F.; Binnemans, K.; Van Deun, R.; Bruce, D.W. *Mol. Cryst. Liq. Cryst*. **2001**, *364*, 745–752.
[42] Geary, W.G. *Coord. Chem. Rev*. **1971**, *7*, 81–122.
[43] Farmer, R.L.; Urbach, F.L. *Inorg. Chem*. **1974**, *13*, 587–590.
[44] Pasquali, M.; Marchetti, F.; Merlino, S. *J. Chem. Soc., Dalton Trans*. **1977**, 139–144.
[45] Serrette, A.; Carroll, P.J.; Swager, T.M. *J. Am. Chem. Soc*. **1992**, *114*, 1887–1889. Corrigendum *J. Am. Chem. Soc*. **1993**, *115*, 11656.
[46] Campillos, E.; Marcos, M.; Omenat, A.; Serrano, J.L. *J. Mater. Chem*. **1996**, *6*, 349–355.
[47] Iglesias, R.; Marcos, M.; Serrano, J.L.; Sierra, T.; Perez-Jubindo, M.A. *Chem. Mater*. **1996**, *8*, 2611–2617.
[48] Zheng, H.; Lai, C.K.; Swager, T.M. *Chem. Mater*. **1995**, *7*, 2067–2077.
[49] Kumari, S.; Singh, A.K.; Kumar, K.R.; Sridhar, B.; Rao, T.R. *Inorg. Chim. Acta* **2009**, *362*, 4205–4211.
[50] Lakowicz, J.R. *Principle of Fluorescence Spectroscopy*; Kluwer Academic/Plenum Publishing Corporation: New York, 2006.
[51] Asefa, A.; Singh, A.K. *J. Luminescence* **2010**, *130*, 24–28.
[52] Jozefowicz, M.; Heldt, J.R. *J. Fluorescence* **2011**, *21*, 239–245.
[53] Atsbeha, T.; Mohammed, A.M.; Abshiro, M.R. *J. Fluorescence* **2010**, *20*, 1241–1248.
[54] Dierking, I. *Textures of Liquid Crystals*; Wiley-VCH GmbH&Co: Weinheim, 2003.
[55] Galyametdinov, Y.G.; Ivanova, G.I. *Izv. Akad. Nauk. SSSR, Ser. Khim*. **1989**, *9*, 1997–2001.
[56] Galyametdinov, Yu.G.; Ivanova, G.I.; Bikchantaev, I.G.; Tinchurina, L.M.; Ovchinnikov, I.V. *Izv. Akad. Nauk. SSSR, Ser. Khim*. **1989**, *12*, 2833–2838.
[57] Keller, P.; Liebert, L. *Solid State Phys. Suppl*. **1978**, *14*, 19.
[58] Artigas, M.; Marcos, M.; Melendez, E.; Serrano, J.L. *Mol. Cryst. Liq. Cryst*. **1985**, *130*, 337–347.
[59] Lai, C.K.; Leu, Y.F. *Liq. Cryst*. **1998**, *25*,689–698.

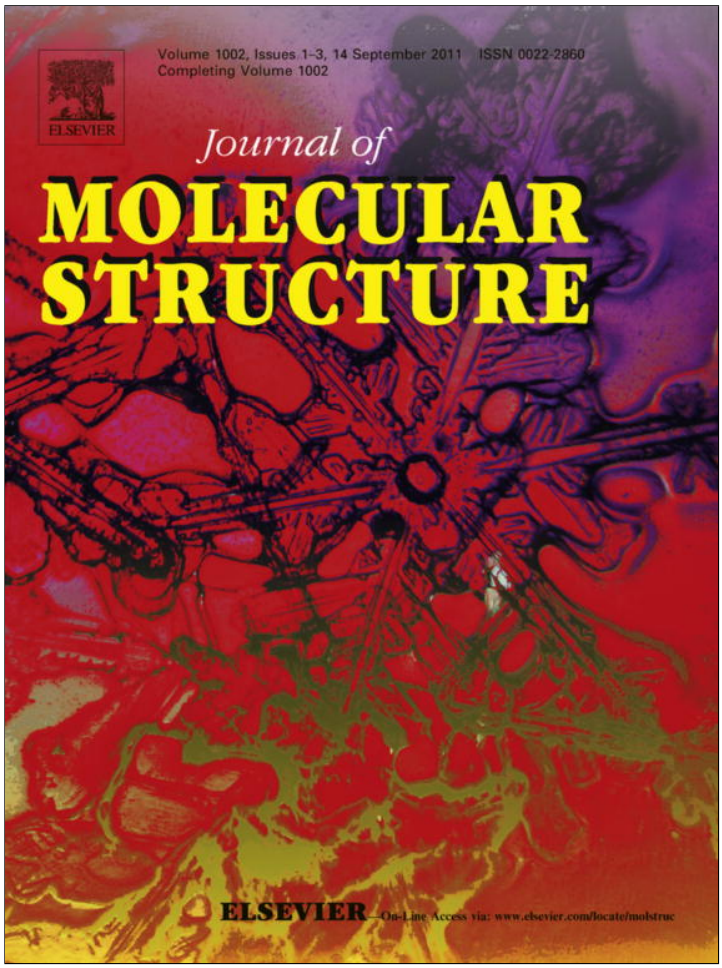

Journal of Molecular Structure 1002 (2011) 135–144

Contents lists available at ScienceDirect

Journal of Molecular Structure

journal homepage: www.elsevier.com/locate/molstruc

Synthesis and properties of copper (II), oxovanadium (IV) and gadolinium (III) complexes derived from polar Schiff's bases

Lopamudra Chakraborty, Nirmalangshu Chakraborty, Atiqur Rahman Laskar, Manoj Kumar Paul, Nandiraju V.S. Rao *

Chemistry Department, Assam University, Silchar 788 011, Assam, India

ARTICLE INFO

Article history:
Received 1 April 2011
Received in revised form 5 July 2011
Accepted 5 July 2011
Available online 10 August 2011

Keywords:
Metallomesogens
Liquid crystals
Smectic phase
Polar compounds
Schiff's bases

ABSTRACT

The synthesis, liquid crystalline and optical properties of copper (II), oxovanadium (IV) and gadolinium (III) complexes derived from polar Schiff's bases viz., N-(4-n-hexadecyloxysalicylidene)-4′-substituted anilines with methoxy, fluoro and chloro substituents in the 4-position of N-aryl moiety are presented. All the ligands exhibited smectic A phase except methoxy homolog which exhibited nematic phase. Majority of the complexes exhibited smectic A phase with some of them exhibiting smectic E phases. The UV–Visible and photo-luminescent properties of the ligands and complexes are also discussed.

1. Introduction

Metal containing liquid crystals called as metallomesogens have received a lot of attention in the last three decades due to its importance in the basic liquid crystals research as well as its potential utility in industrial, chemical, medical, and sensor applications [1–13]. The nature of metal plays an important role to influence the mesomorphic properties of the organic ligand to which it coordinates. The importance of Schiff bases viz., N-(4-n-alkoxysalicylidene)-4′-n-alkyl(oxy)anilines lies in their rich mesomorphism at ambient temperatures and as well as their suitability for extension with many functional groups [14–16]. Extensive studies are carried out on metallomesogens of d-block elements coordinated to N-(4-n-alkoxysalicylidene)-4′-n-alkyl(oxy)anilines because of the ease of synthesis, stability of the complexes and rich variety of mesophases [10–13]. The incorporation of metal ion with unpaired electrons in these Schiff base ligands can lead to the formation of paramagnetic liquid crystalline (LC) materials. The alignment of paramagnetic LCs possessing large magnetic anisotropy can be realized by small magnetic field strengths. Hence the coordination of paramagnetic lanthanide ions with N-(4-n-alkoxysalicylidene)-4′-n-alkyl(oxy)anilines can generate low molar mass magnetic liquid crystals which possess large magnetic anisotropy. However related studies of the f-block lanthanide ion complexes are relatively limited to N-(4-n-alkoxysalicylidene)-n-alkylamines, **L1-L4** coordinated to lanthanide ions, as shown in Fig. 1 [14–17] apart from few examples of rare-earth containing metallomesogens with other ligands. The first calamitic bidentate salicylideneimine nO(OH)m_{ali}, possessing N-aliphatic moiety based lanthanide complexes was reported in 1991 [14] and a new nomenclature of lanthanidomesogens had been proposed [18–21]. However the efforts in different laboratories [17] to coordinate f-block metals with the salicylideneimine based ligands with an aryl moiety [14–17] on nitrogen atom of the central bridging imine group have been unsuccessful. The difference in basicity of the nitrogens of N-alkyl and N-aryl imines of the ligand to form a zwitter ion led to the coordination of the zwitter ionic N-alkyl imines only to form the lanthanide complexes, while it is not realized with aromatic imines.

N, N′-aromatic donors shown in Fig. 2 [22] viz., 4,7-disubstituted phenanthroline (**L5** and **L6**), or 4,4′-dimethoxy-2,2′-bipyridine (**L7**) coordination with the lanthanide ions was successful, while diethyl-2,2′-bipyridine-4,4′-dicarboxylate (**L8**) did not participate in coordination. Hence it has been accounted for an electronic destabilization of the ester groups on the aromatic bipyridine core, which is associated with a more flexible conformation with respect to the phenanthroline to make this ligand not compatible for chelation with a lanthanide ion of any size. In fact the influence of the substituents on the basicity and the coordination ability of the N, N′-aromatic ligands, viz., 4,4′-dimethoxy-2,2′-bipyridine, (**L3**) the bipyridine bearing a methoxy group in 4,4′-position, produced high yields of the complexes reflecting the dramatically enhanced activation towards coordination.

* Corresponding author. Tel.: +91 9435522541; fax: +91 3842270806.
E-mail address: drnvsrao@gmail.com (N.V.S. Rao).

0022-2860/$ - see front matter © 2011 Elsevier B.V. All rights reserved.
doi:10.1016/j.molstruc.2011.07.010

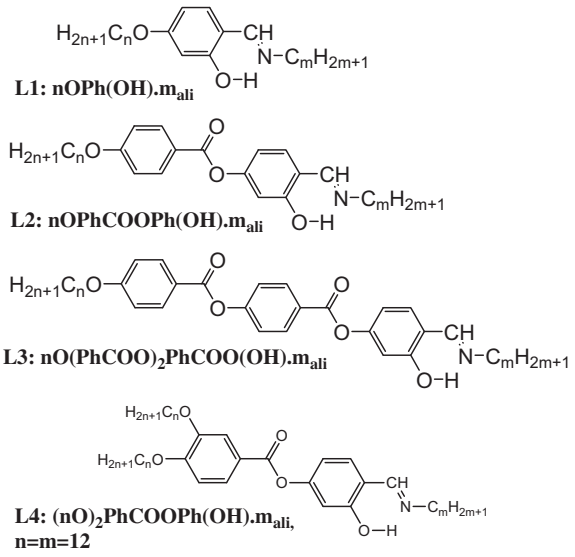

Fig. 1. Molecular structure of Schiff's base ligands studied extensively for complexation [14–17].

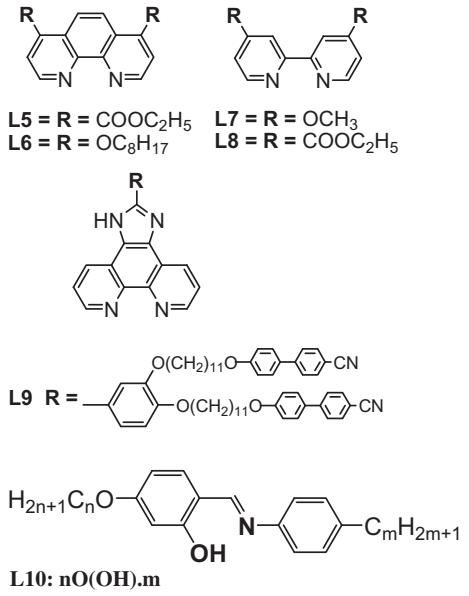

Fig. 2. Molecular structure of N, N′-aromatic donors for complexation.

However modification of the phenanthroline ligand (**L9**) in 5,6-positions fused with a substituted imidazo ring led the realization of nematic phase [23].

Hence the design and synthesis of lanthanide containing liquid crystals viz., salicylideneimine based promesogenic ligands, with a polar group substituted in an aryl moiety on nitrogen atom of the central bridging imine group, to coordinate with f-block metals presents a special experimental challenge. Our previous attempts were successful in reporting the complexation of different lanthanide ions with N-(4-n-alkoxysalicylidene)-4′-n-alkylanilines, **L10** [24,25]. The lanthanide complexes in general exhibited SmA phase but some of them exhibited columnar phases [25,26] depending on the aliphatic chains component in the ligand. In continuation of earlier work we report here the complexation of different lanthanide (III) ions with N-(4-n-hexadecyloxysalicylidene)-4′-substituted-anilines, the substituent being a polar group in N-aryl moiety, characterization of mesomorphism of the ligands as well as complexes and their spectroscopic characteristics. A comparison with complexes of d-block elements is also presented.

2. Results and discussion

The synthesis of ligands viz., N-(4-n-decyloxysalicylidene)-4′-substituted-(methyloxy, chloro and fluoro)-anilines (hereafter abbreviated as 16O(OH)X where X = H, OMe, F, Cl) and their Cu (II) and VO (IV) (*d*-block) complexes and Gd (III) (f-block) complexes as detailed in Scheme 1, was carried out following the procedure described in experimental section. Sm(III) and Pr(III) complexes were also synthesized and characterized by IR, UV–Vis and fluorescence studies.

Elemental analysis of the ligands and copper (II) and oxovanadium (IV) complexes were consistent with their proposed molecular formulas (Table 1). Elemental analysis of lanthanide complexes revealed that the stoichiometry is $\{[Ln(LH)_2L](NO_3)_2\}$, where Ln = Gd, and LH = **2, 3** and **4**. We investigated the ionic conductivity of solutions of the ligand **3** [16O(OH)F], $c = 1.0 \times 10^{-4}$ M and **3-Gd** (Gadolinium complex, $c = 1.0 \times 10^{-3}$ M) in double distilled and dried N,N′-dimethylformamide (DMF). The conductivity values (Table 2) inferred that the ligand is a non-electrolyte. However the **3-Gd**, (Gd complex) is a 2:1 electrolyte with the two nitrate ions participation from outer coordination sphere [27] confirming the elemental analysis data. The room temperature infrared spectra of the ligands **1, 2, 3** and **4** exhibited characteristic bands (ν(C═N)) at 1622–1627 cm^{-1}. The C═N stretching vibration is shifted to lower frequencies for the copper (II) (1608 cm^{-1}) and oxovanadium (IV) (1608–1610 cm^{-1}) complexes compared to that of free ligands. This reflects the azomethine N atom is involved in metal-nitrogen bond formation. The oxovanadium (IV) complexes exhibit a stretching band at around 966–987 cm^{-1} assigned to ν(V—O) suggesting that these complexes have a monomeric structure [28–31].

However the infrared spectra of lanthanide (III) complexes exhibited characteristic C═N stretching vibration (ν(C═N)) at ~1640 ± 5 cm^{-1} and 1616–1622 cm^{-1} (Table 1) for the complexes (Representative IR spectra of the complex **2-Gd** and **3-Gd** are shown in Fig. 3.), apart from the characteristic bands of aromatic ring (C═C), Ar(C—H), CH_3, and CH_2 vibrations. These two bands confirm two types of coordination one through the oxygen atom and another through the nitrogen atom. The band at ~1616–1622 cm^{-1} reflects the participation of azomethine N atom in metal-nitrogen bond formation in the case of toluidine (**2-Gd**) and chloro complexes (**4-Gd**). However the absence of C═N stretching vibration for fluoro complex **3-Gd** at ~1620 cm^{-1} reflects the absence of metal-nitrogen coordination bond formation. The weak O—H stretching vibration of the ligand at 2870–2850 cm^{-1}, is overlapped by the CH modes in the lanthanide complexes reflecting the N—H vibration of the protonated nitrogen atom in C═N$^+$H as well as the participation of hydrogen atom in the intramolecular hydrogen bonding with the phenolic oxygen atom as reported earlier [32]. This abnormal behavior may be due to coordination of the metal through O-atom of the ligand only, the proton of the O-atom migrate to the N-atom of the imine moiety which may -lead to formation of zwitter ion (C═N$^+$—H) of ligand. The observed vibrations of two bands at 1635–1645 cm^{-1} and ~1620 cm^{-1} for the complex $Gd[(L^4H)_2(L)]\cdot(NO_3)_2$, are due to two types of CH═N stretching and compression vibrations. One of these is the elongated stretching viz., exactly opposite with an increase in the imine **C═N** stretching vibration of the complex (at 1635–1645 cm^{-1}) in the infrared spectra when compared to the stretching vibration in the free Schiff base ligand, while the other one is a compressed imine bond appearing at a lower value of 1620 cm^{-1}. The vibration at higher

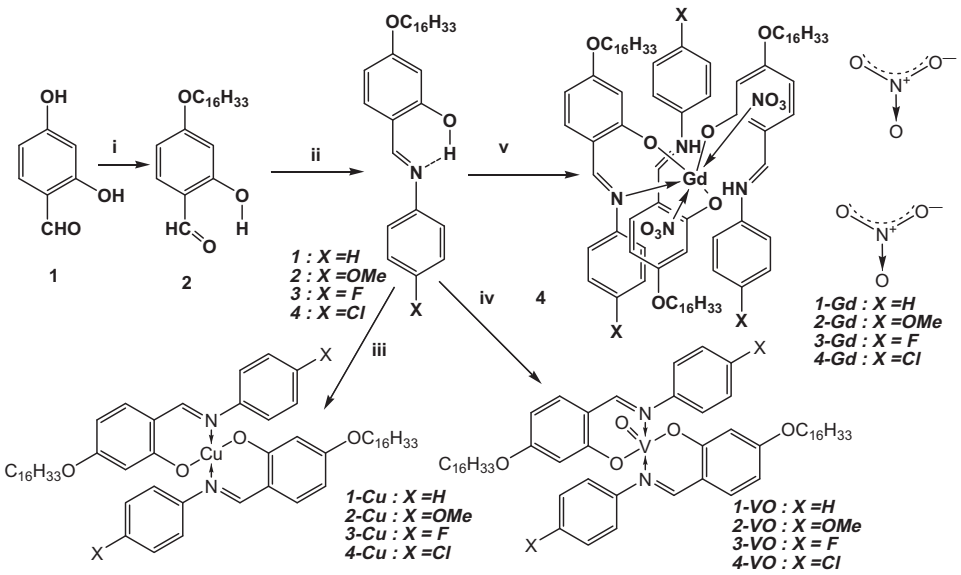

Scheme 1. $C_{16}H_{33}Br$, $KHCO_3$, KI, dry acetone, reflux, 40 h ii. 1 = aniline, 2 = 4-Anisidine, 3 = 4-fluoroaniline, 4 = 4-chloroaniline glacial AcOH, absolute EtOH, Reflux, 4 h iii. $Cu(OAc)_2.H_2O$, EtOH; iv. $VOSO_4.5H_2O$, MeOH, TEA; v. $Gd(NO_3)_3$; Acetonitrile, Reflux, 4 h. For the sake of clarity the coordination of oxygen atoms of nitrate ion is shown through nitrate ions.

Table 1
Elemental analysis data (calculated values in parentheses) and yields of the complexes.

Compound	Molecular formula	C (%)	H (%)	N (%)	Yield (%)	IR data (cm^{-1})
2	$C_{30}H_{45}NO_3$	77.25 (77.04)	9.59 (9.70)	3.09 (2.99)	71	1627
2-Cu	$C_{60}H_{88}CuN_2O_6$	72.55 (72.29)	8.76 (8.90)	2.67 (2.81)	65	1608
2-VO	$C_{60}H_{88}N_2O_7V$	72.14 (72.04)	8.65 (8.87)	2.65 (2.80)	58	1608, 987
2-Gd	$C_{90}H_{134}GdN_5O_{15}$	65.21 (64.22)	7.88 (8.02)	4.39 (4.16)	45	1641,1622
3	$C_{29}H_{42}FNO_2$	76.29 (76.44)	9.19 (9.29)	2.99 (3.07)	74	1625
3-Cu	$C_{58}H_{82}F_2CuN_2O_4$	71.15 (71.61)	8.39 (8.50)	3.01 (2.88)	71	1608
3-VO	$C_{58}H_{82}F_2N_2O_5V$	71.35 (71.36)	8.58 (8.47)	2.65 (2.87)	67	1608, 970
3-Gd	$C_{90}H_{125}F_3GdN_5O_{12}$	62.42 (63.44)	7.21 (7.65)	4.01 (4.25)	42	1645
4	$C_{29}H_{42}ClNO_2$	73.98 (73.78)	8.91 (8.97)	2.88 (2.97)	65	1627
4-Cu	$C_{58}H_{82}Cl_2CuN_2O_4$	69.65 (69.26)	8.29 (8.22)	2.55 (2.79)	61	1608
4-VO	$C_{58}H_{82}Cl_2N_2O_5V$	69.43 (69.03)	8.25 (8.19)	2.59 (2.78)	55	1610, 966
4-Gd	$C_{90}H_{125}Cl_3GdN_5O_{12}$	62.55 (61.59)	7.65 (7.43)	4.31 (4.13)	42	1635, 1620

Table 2
Electrical conductivity of the compound 3, its Gd(III) complex and $Gd(III)NO_3 \cdot 6H_2O$. Concentration is 1×10^{-3} M.

	Molar conductivity ($ohm^{-1}\ cm^2\ mol^{-1}$)		
Compound	N,N′-Dimethylformamide	Ethanol	Acetonitrile
3: 16O(OH)F :L^3H	15	15	9
3-Gd: [$Gd(L^3H)_2L^3](NO_3)_2$	185	92	165
$Gd(NO)_3.6H_2O$	205	83	30

frequency (1635–1645 cm^{-1}) is due to the complexation of oxygen atom with the rare earth ion. This is exactly opposite to the observation of imine **C═N** stretching vibration of the copper (II) and VO complexes of **2** and **4** [$Cu(L^4)_2$ at 1608–1610 cm^{-1}] in the infrared spectra which is lower than the imine **C═N** stretching vibration of the free ligand L^4H (1627 cm^{-1}), indicating a decrease in strength of the double bond character of **C═N** bond. Hence the lower value of 1620 cm^{-1} clearly indicated similar type of coordination of the complexation as in copper complexes which take place through the deprotonated phenolic oxygen and azomethine nitrogen atoms. The phenolic C—O stretching vibration, which is observed in the Schiff base ligands around 1290 cm^{-1}, overlaps in the metal complexes with a vibration due to the nitrate groups. The four bands in the IR spectra of all the lanthanide complexes (only Gd(III) complexes are reported here while Pr(III) and Sm(III) complexes also gave identical spectra) recorded at 1475, 1286, 1122 and 827 cm^{-1} can be assigned to the vibrational modes of the coordinated (C_{2V}) nitrate group reflecting the vibrations of ν_4, ν_1, ν_2, and ν_6 are respectively. Even though it may be assumed that mono dentate nitrate group participates in coordination, the magnitude of splitting in the peak positions of the bands of ν_4 and ν_1 (186 cm^{-1}) characterize the coordination of nitrate group as bidentate rather than mono dentate. The additional bands observed ~1384 cm^{-1} suggests the presence of non-coordinated nitrate groups present in the complex.

3. Thermal behavior: DSC and thermal microscopy

3.1. Mesomorphic behavior of ligands

The polarized optical microscopy was performed to confirm the transition temperatures obtained by DSC studies and to find out

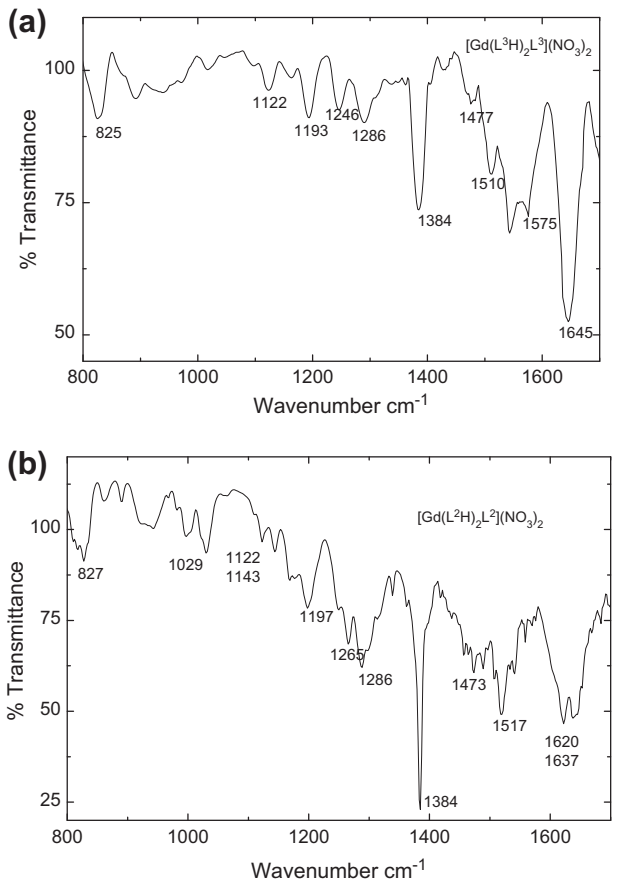

Fig. 3. FTIR spectra of gadolinium (III) complexes of (a) fluoro and (b) methoxy homologs.

the type of liquid crystalline phases present in the studied materials. The liquid crystalline phases, phase transition temperatures, enthalpy and entropy associated with the phase transitions of the ligands and complexes are summarized in Table 3. All the compounds exhibited strong birefringence and fluidity in the temperature range characteristic of mesomorphic behavior between the endothermic or exothermic peaks recorded in DSC thermograms in the heating or cooling cycle respectively. All the ligands exhibit mesomorphism. The compound **1** without any substituent on N-aryl moiety exhibited focal conic fan texture of SmA phase of 0.1 °C. The compound 16O(OH)OMe (**2**) with methoxy group exhibit schlieren texture characteristic of nematic phase (Fig. 4a) while the other two compounds **3** and **4** with a polar substituent (F or Cl respectively) displayed focal conic fan texture characteristic of SmA phase (Fig. 4b,c). The observed mesophase thermal range (ΔT) is 15 °C for 16O(OH)OMe (**2**), 2.3 °C and 34 °C in case of fluoro (**3**) and chloro (**4**) homologs respectively. A representative DSC spectrum of fluoro homolog **3** is displayed in Fig. 5. In a previous report [33–35] on lower homologs of similar compounds viz., 7O(OH)X, where X = H, OMe, F and Cl, 7O(OH)H do not exhibit LC behavior while OMe ($\Delta T \sim 16.9$ °C) exhibits nematic phase, fluoro ($\Delta T \sim 0.5$ °C) and chloro ($\Delta T \sim 50$ °C) homologs exhibit SmA phases. A comparison of transition temperatures between the two homologs (Table 4) revealed the increase in melting/crystallization temperatures. The increase in thermal ranges can be explained as follows.

The thermal stability of the mesophase in these compounds is determined by the anisotropy of the contribution of the polarizability of X, the electronic structure of the N-phenyl moiety under the influence of the substituent inductive and resonance contributions and the associated change in the geometric anisotropy of the molecule. The contribution of substituent polarizability to the total polarizability and polarity of the molecule and the changes induced by the substituent X in the π-conjugation of —CH═N—C_6H_4X fragment as well as the conformation of the molecule determine the thermal stability of the compounds. The methoxy group in N-phenyl moiety with stronger donor properties reduces the effect of π-conjugation of —CH═N—C_6H_4X which is further augmented by the intramolecular H-bonding manifested between the proton of ortho-hydroxyl group in aldehyde moiety and the lone pair of the electrons on the nitrogen atom in azomethine unit. Both these effects contribute to increased planar conformation of the molecule in these compounds in comparison to the noncoplanarity of the phenyl rings on both sides of azomethine linkage in Schiff bases. Hence the apparent stronger dispersion attraction between the planar molecules is reflected in the increase of crystal-mesophase transition temperature when H is replaced by methoxy group.

3.2. Mesomorphic behavior of complexes

All the complexes exhibit smectic A phase while an additional smectic E phase is exhibited by the Cu(II) complexes of fluoro and chloro compounds and all the Gd(III) complexes. The characteristic textures exhibited by the complexes of compounds **2**, **3** and **4** are displayed in Figs. 6–8 respectively. The optical texture of SmE phase with striations across the fans can be seen in for Gd(III) complexes (Figs. 6d and 7d) and for Cu(II) complexes (Fig. 8b). In an earlier report Galyametdinov et al. [35] observed an increase in mesomorphic range of fluoro homolog [N-(4-n-heptyloxysalicylidene)-4′-fluoroaniline] on complexation while a substantial decrease in mesomorphic range of chloro and methoxy homologs. However, in the present work with the increase in carbon chain length from C_7 to C_{16}, enhanced width of mesomorphic range (Table 4) in all the complexes of Cu(II), VO(IV) and Gd(III) than that of the ligands is observed. Hence we rationalize that competing influence between the alkyl chain length and electronic nature of the substituent plays an important role in the mesomorphism of these complexes.

The differential scanning spectra of the fluoro complexes viz., **3-Cu**, **3-VO** and **3-Gd** is displayed in Fig. 9a–c respectively. The mesomorphic thermal range increased from 30.1 °C for copper complex to 103.3 °C and 138.4 °C for oxovanadium and gadolinium complexes, respectively. The predominant influence of metal ion complexation in the manifestation of mesomorphism of a polar ligand is augmented by the suitable end alkyl chain length to enhance the mesomorphic range. The larger width of mesomorphic range (92–136 °C in cooling cycle) particularly in oxovanadium complexes than the copper complexes is surprising and it may be due to electronic interactions of VO moiety as well as functional groups rather than the steric hindrance of the VO group. In general all the Cu(II), VO(IV) and Gd(III) complexes exhibited focal conic fan texture characterizing the phase as SmA, while the Cu(II) and gadolinium (III) complexes of fluoro and chloro compounds exhibited additional phase texture resembling SmE phase. In contrast to the ligands the complexes exhibit wide mesomorphic ranges. The electronic nature and size of the substituent can also influence the molecular structure of the ligands and complexes and thereby affects mesomorphism. It is apparent from the DSC and POM investigations that the width of the mesomorphic range is substantially influenced by the nature of substituent as well as the metal ion in corresponding complexes. These results are in good agreement with the earlier reported results on similar compounds where the alkyloxy chain is heptyloxy homolog [33]. The only difference is the enantiotropic mesophases are observed with the increase in chain length of salicylidene moiety.

Table 3
Phase transition temperatures, associated enthalpy and entropy changes data for the ligands and complexes.

	Compound	Transition	T (°C)	ΔH (kJ mol^{-1})	ΔS (J mol^{-1} K^{-1})	ΔT (°C)
1	16O(OH)H = (L^1H)	K-I	79.4	66.1	187.6	
		I-SmA	67.3	22.8	67	0.1
		SmA-K	67.2	34.4	101.1	
1-Cu	Cu(L^1)$_2$	K-I	111.6	60.1	157.1	–
		I-K	77.8	80.2	228.6	
1-VO	VO(L^1)$_2$	K-I	106.6	3.63	9.56	–
		I-K	75.8	2.47	18.5	
2	16O(OH)O1 = (L^2H)	K-N	100.5	62.77	185.3	
		N-I	102.2	1.16	3.09	1.7
		I-N	101.3	1.51	4.03	15.0
		N-K	86.3	58.9	164.0	
2-Cu	Cu(L^2)$_2$	K1-K	118.5	18.9	48.5	
		K-SmA	122.8	47.3	119.5	
		SmA-I	141.8	7.01	16.8	19.0
		I-SmA	141.0	7.42	17.9	60.2
		SmA-K	80.8	54.9	155.3	
2-VO	VO(L^2)$_2$	K-SmA	99.3	79.3	213.1	
		SmA-I	195.0	5.64	12.0	95.7
		I-SmA	189.1	3.54	7.66	136.0
		SmA-K	53.02	13.3	40.8	
2-Gd	[Gd(L^2H)$_2$$L^2$](NO$_3$)$_2$	K-SmE	107.7	9.9	26.1	
		SmE-SmA	127.5	12.4	31.1	
		SmA-I	194.3	31.2	66.9	86.6
		I-SmA	192.1*	–		97.1
		SmA-SmE	126.1*	–		
		SmE-K	95.1*	–		
3	16O(OH)F = (L^3H)	K1-K	78.9	0.69	1.96	
		K-I	83.6	56.1	157.4	–
		I-SmA	74.9	3.78	10.8	2.3
		SmA-K	72.6	55.0	159.2	
3-Cu	Cu(L^3)$_2$	K-SmE	119.1	49.5	126.4	
		SmE-SmA	120.8	2.99	7.60	
		SmA-I	125.7	5.05	12.6	6.6
		I-SmA	124.3	5.10	12.8	30.1
		SmA-SmE	97.8	3.32	8.90	
		SmE-K	94.2	60.5	164.7	
3-VO	VO(L^3)$_2$	K-SmA	122.2	76.4	193.4	
		SmA-I	161.9	11.1	25.6	39.7
		I-SmA	160.4	10.8	25.1	103.3
		SmA-K	57.1	21.0	63.8	
3-Gd	[Gd(L^3H)$_2$$L^3$](NO$_3$)$_2$	K-SmE	67.9	12.3	36.2	
		SmE-SmA	139.1*	–	–	
		SmA-I	188.8	10.0	21.7	120.9
		I-SmA	183.5*	–	–	138.4
		SmA-SmE	135.1*	–	–	
		SmE-K	45.1*	–	–	
4	16O(OH)Cl = (L^4H)	K-SmA	87.9	66.9	185.4	
		SmA-I	106.4	5.8	15.2	19.5
		I-SmA	105.9	5.43	14.3	34.0
		SmA-K	71.9	67.7	196.5	
4-Cu	Cu(L^4)$_2$	K-SmE	117.4	36.9	94.6	
		SmE-SmA	172.1	19.1	42.9	
		SmA-I	179.6	7.52	16.6	62.2
		I-SmA	175.6	5.22	11.6	67.6
		SmA-SmE	144.4	22.9	55.0	
		SmE-K	108.0	23.1	60.7	
4-VO	VO(L^4)$_2$	K-SmA	115.5	32.3	83.4	
		SmA-I	144.7	6.40	15.3	29.4
		I-SmA	143.4	5.28	12.7	92.6
		SmA-K	50.8	11.8	36.5	
4-Gd	[Gd(L^4H)$_2$$L^4$](NO$_3$)$_2$	K-SmE	87.5	47.6	132.0	
		SmE-SmA	92.6	2.86	7.8	
		SmA-I	163.0	6.3	14.5	75.5
		I-SmA	161.1*	–	–	
		SmA-SmE	82.5*	–	–	
		SmE-K	45.2*	–	–	

* Indicates the POM observed values.

4. Optical absorption and emission studies

The UV–Visible absorption (Table 5) and fluorescence spectroscopic properties of compound **4** and its complexes in chloroform solution with concentration ($c = 1 \times 10^{-5}$), Fig. 10 (with chloroform as the solvent being chosen to maximize the molecular solubility) were studied to obtain the information regarding absorption and emission maxima, and the Stokes shift of fluorescence. The green

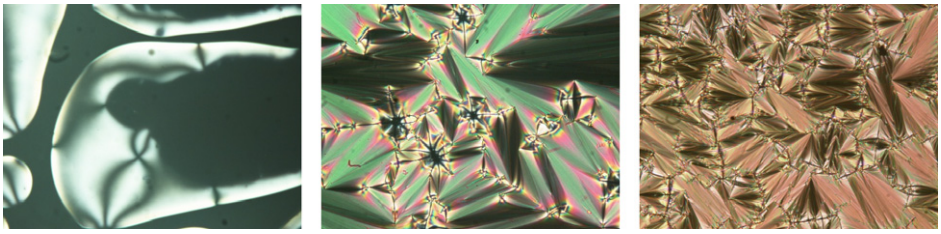

(a) Schlieren texture of nematic phase of **2** at 100.6 ^{0}C

(b) Focal conic texture of SmA phase of **3** at 74 ^{0}C

(c) Focal conic texture of SmA phase of **4** at 105.4 ^{0}C

Fig. 4. (a) Schlieren texture of nematic phase of **2** at 100.6 °C, (b) focal conic texture of SmA phase of **3** at 79 °C, and (c) focal conic texture of SmA phase of **4** at 105.4 °C.

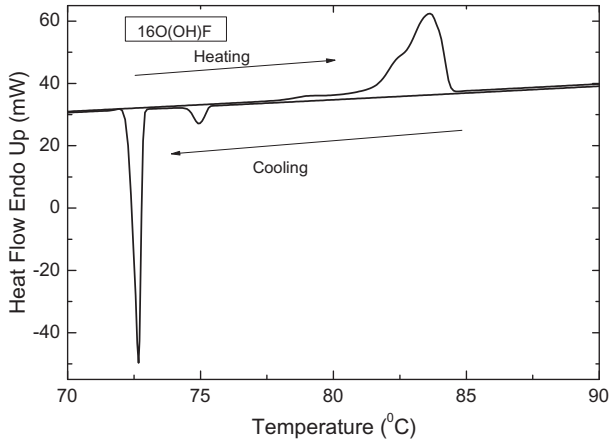

Fig. 5. DSC spectrum of the compound **3**.

fluorescence of **4-Gd** when exposed to UV light is shown in Fig. 11. The absorption maxima of the lowest optical transition were observed approximately at 342–355 nm for compound 4 (and other ligands as well) (~3.6 eV, $\sim\varepsilon$ = 80,000–146,000 L mol^{-1} cm^{-1}) with two other maxima in at 245 nm and 300 nm. The extended conjugated π-system is reflected in the electronic absorption spectrum. The electronic properties of these systems are dominated by the donor–acceptor-substituted organic chromophore ligand bands with a noticeable shift for the d-block complexes. However no noticeable shift to lower or higher energy levels for the lanthanide complexes is observed indicating the absence of crystal field effect upon the inter-electronic repulsion between the *4f* electrons of the metal ion. These absorption bands with large molar absorption coefficients reflects the π–π* transition of the highly π-conjugated system of the ligand surrounding the metal ion core. Luminescence studies of metallomesogens are scanty [36] and luminescent studies on the ligand and complexes were carried out in solution and thin film of the solid phases. The most important features of the photoluminescence emission spectra of the lanthanide metallomesogens and ligands in chloroform solution at different concentrations and in thin solid film are the large Stokes shifted emission of ~174 nm for **4-Gd** complex and ~122–129 nm (Fig. 10) and broad emission band with maxima in the vicinity of ~520 nm and ~471 nm for **4-Gd** and **4-Pr** complexes respectively. The Stokes shift, which reflects the structural relaxation of the excited molecule, is in the range reported for other metallomesogens [37–39] but significantly larger than the reported push–pull systems [40–44] exhibiting liquid crystal behavior, confirmed the molecular conformational changes upon excitation. Hence it can be assigned to the ligand–ligand charge transfer transition due to the presence of phenyl rings in the ligands and also indicative of phosphorescence. Further studies are in progress to change the design of the ligand to promote metal centered absorption and emission.

5. Conclusions

The synthesis of *d*- and f-block metal complexes of N-(4-n-hexadecyloxysalicylidene)-4′-substituted anilines, with the polar substituents (Cl and F), exhibiting mesomorphism had been successfully achieved. Proper choice of end alkyl chain length can influence the manifestation of mesomorphism in ligands as well as their complexes. Hence competing influence between the alkyl chain length and electronic nature of the substituent plays an important role in the mesomorphism of these complexes. In particular the special experimental challenge of synthesis of lanthanide containing liquid crystals viz., salicylideneimine based promesogenic ligands, with *a polar group substituted in an aryl moiety on nitrogen atom of the central bridging imine group* is fulfilled. These complexes possess large thermotropic mesomorphic range exhibiting SmA and SmE phases. The major advantage of Lanthanide containing metallomesogens is intense luminescence characteristics as well as large mesomorphic range close to ambient temperature. The studies on magnetic anisotropy of these complexes is still to be explored and further work is in progress to synthesize stable room temperature lanthanidomesogens exhibiting nematic and smectic phases by suitable changes in the end alkyl chains, substituents in the aromatic core and counter-ions.

Table 4
Comparison of transition temperatures and mesomorphic range in °C of ligands and complexes.

		H	OMe	Me	F	Cl
Melting point of 7O(OH)X	Heating	50.9	90.0	64.9	73.0	72.0
Melting point/crystallization of 16O(OH)X	Heating	79.4	100.5	84.6	83.6	87.9
	Cooling	–	102.2	84.6	83.6	106.4
Δ*T* of 16O(OH)X		0.1	15.0	1.5	2.3	34.0
Cu(II) complexes of 16O(OH)X		–	60.2	3.7	30.1	67.6
VO(IV) complexes of 16O(OH)X		–	136.0	33.1	103.3	92.6

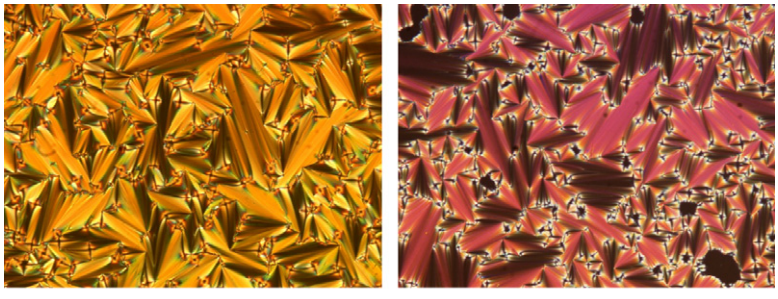

(a) SmA phase texture of **2-Cu**, $[L^2]_2Cu$, at 137.2 ^0C

(b) SmA phase texture of **2-VO**, $[L^2]_2VO$ at 127.2 ^0C

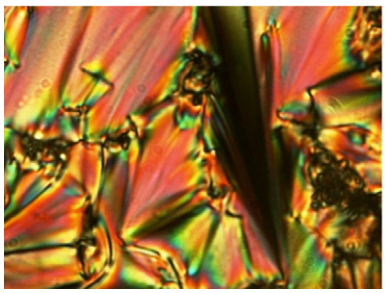

(c) SmA phase texture of **2-Gd** at 192 ^0C

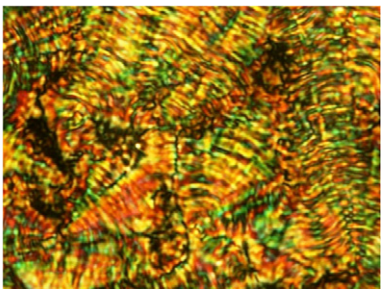

(d) SmE phase texture of **2-Gd** at 125 ^0C

Fig. 6. Focal conic fan textures exhibited by complexes of compound **2**: **2-Cu, 2-VO and 2-Gd**.

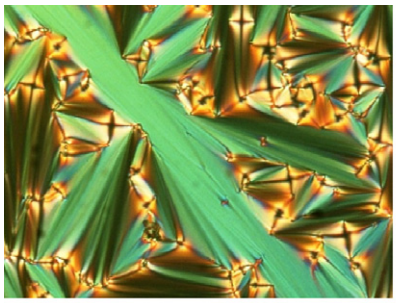

(a) SmA phase texture of **3-Cu**, $[L^3]_2Cu$ 119 ^0C

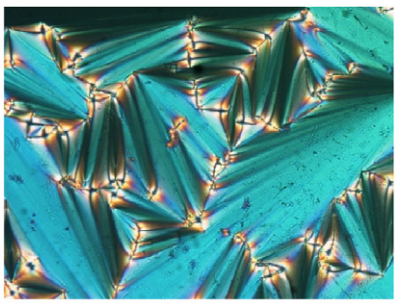

(b) SmA phase texture of **3-VO**, $[L^3]_2VO$ 151.9 ^0C

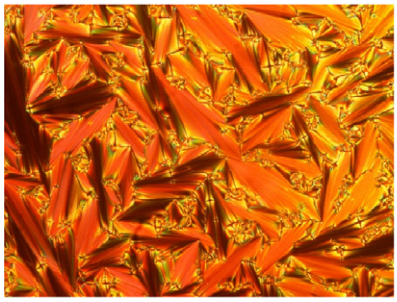

(c) SmA phase texture of **3-Gd**, $[Gd(L^3H)_2L^3](NO_3)_2$ 182.6 ^0C

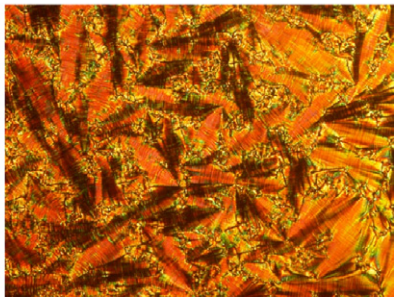

(d) SmE phase texture of **3-Gd**, $[Gd(L^3H)_2L^3](NO_3)_2$ 130 ^0C

Fig. 7. Focal conic fan textures exhibited by complexes of compound **3**: **3-Cu, 3-VO and 3-Gd**.

6. Experimental

All the chemicals were procured from M/s Alfa Aesar, Tokyo Kasei Kogyo Co. Ltd. or Lancaster chemicals, Sigma–Aldrich Chemicals. The solvents and reagents are of AR grade and were distilled and dried before use. Microanalysis of C, H and N elements were determined on Carlo-Erba 1106 elemental analyzer. IR spectra were recorded on a Shimadju FT-IR-prestige-21spectrometer (ν_{max}

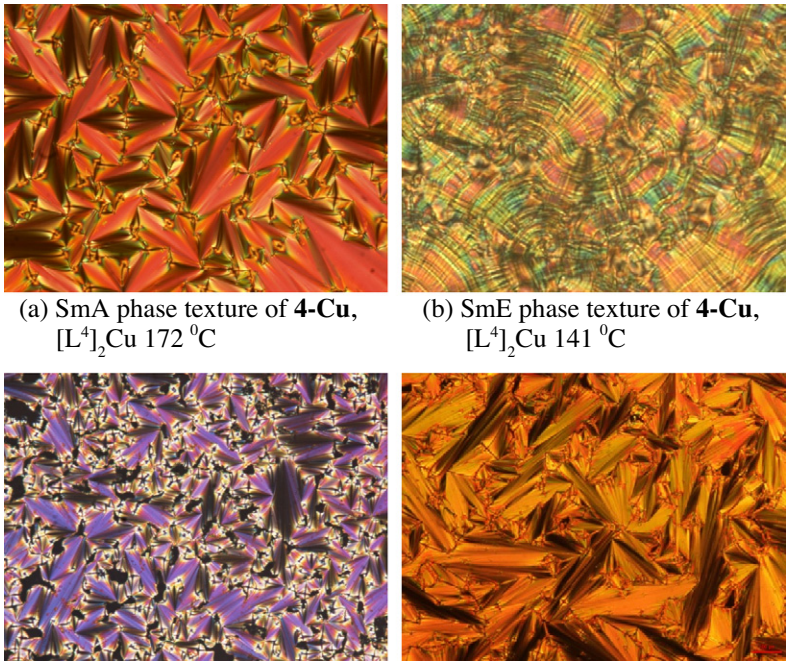

(a) SmA phase texture of **4-Cu**, $[L^4]_2Cu$ 172 ^0C

(b) SmE phase texture of **4-Cu**, $[L^4]_2Cu$ 141 ^0C

(c) SmA phase texture of **4-VO**, $[L^4]_2VO$ 126.4 ^0C

(d) SmA phase texture of **4-Gd** $[Gd(L^4H)_2L^4](NO_3)_2$ 132 ^0C

Fig. 8. Focal conic fan textures exhibited by complexes of compound **4: 4-Cu, 4-VO and 4-Gd**.

in cm^{-1}) over the 400–4000 cm^{-1} spectral range in KBr pellets. The ^1H NMR spectra of all the organic ligands were recorded in $CDCl_3$ solution on a JEOL AL300 FTNMR spectrometer. Conductivity measurements were performed in DMF solution 10^{-3} M on a Systronics CM304 conductivity meter. Chemical shifts are reported in parts per million (δ) relative to tetramethylsilane (TMS) as internal standard. The phase transition temperatures and associated enthalpies were recorded with a heating and cooling rate of 5 °C/min using differential scanning calorimetry (DSC) (Perkin-Elmer Pyris-1 system). The DSC apparatus was calibrated with indium (156.6 °C, 28.4 J/g) and tin (232.1 °C, 60.5 J/g). The liquid crystalline properties of the different phases exhibited by the ligands and complexes were observed and characterized using polarizing microscope (Nikon optiphot-2-pol attached with hot and cold stage HCS302, with STC200 temperature controller configured for HCS302 from INSTEC Inc. USA). UV visible absorption spectra of the compounds in $CHCl_3$ at different concentrations were recorded on a Shimadzu UV-1601PC spectrophotometer (λ_{max} in nm). Fluorescence spectra were recorded with a Shimadju RF-5301PC spectroflouorometer with 150 W xenon lamp as the excitation source.

7. Preparation of ligands and metal complexes

Synthesis of the Schiff bases: The free ligands were synthesized following a well known procedure [45–48] by refluxing a mixture of ethanolic solution of 1 mmol of the 4-n-hexadecyloxysalicylaldehyde with 1 mmol of appropriate amine and few drops of glacial acetic acid as catalyst for 3 h. The precipitated product was purified by repeated recrystallization from absolute ethanol till constant clearing temperatures are achieved (yield 65–75%).

Synthesis of aldehyde: 4-n-hexadecyloxy salicylaldehyde was synthesized as described earlier [46–48] using modified Williamson's method by refluxing 1 mmol of 1-bromohexadecane and 1 mmol of 4-hydroxysalicylaldehyde in the presence of $KHCO_3$ (1 mmol) as base in dry acetone. The product was purified by column chromatography using hexane as eluent.

Preparation of the metal complexes: The synthesis of copper (II) complexes was carried out by refluxing the mixture consisting of slowly added ethanolic copper (II) acetate $[Cu(OAc)_2 \cdot H_2O]$ (1 mmol) solution (20 ml) to a hot solution of the appropriate ethanolic imine (2 mmol) solution (~50 ml) for 2 h. The solution was cooled to room temperature and filtered to yield the brown copper (II) complexes which were subsequently recrystallized from a mixture of ethyl acetate and ethanol.

Oxovanadium (IV) complexes were prepared by refluxing the mixture consisting of slowly added 20 ml of methanolic vanadium (IV) oxide sulfate ($VOS0_4 \cdot 5H_2O$) (1 mmol) solution to a hot solution of the appropriate imine (2 mmol) in methanol (50 ml) in the presence of triethylamine for 4 h. The solution was cooled to room temperature and filtered to yield the green oxovanadium (IV) complexes which were subsequently recrystallized from a mixture of ethyl acetate and ethanol.

Gadolinium (III) complexes were synthesized by refluxing by refluxing the mixture consisting of slowly added gadolinium (III) nitrate $[Gd(NO_3)_3]$ (1 mmol) solution in acetonitrile (20 ml) to a hot solution of the appropriate imine (3 mmol) solution in acetonitrile (~50 ml) for 4 h. The solution was filtered, when it is hot to avoid the impurity of unreacted ligand and to yield the pale yellow precipitate of gadolinium (III) complexes which were washed repeatedly with acetonitrile. The precipitate was dried for further analysis.

Acknowledgement

The authors acknowledge the financial assistance from DAE, DST and UGC.

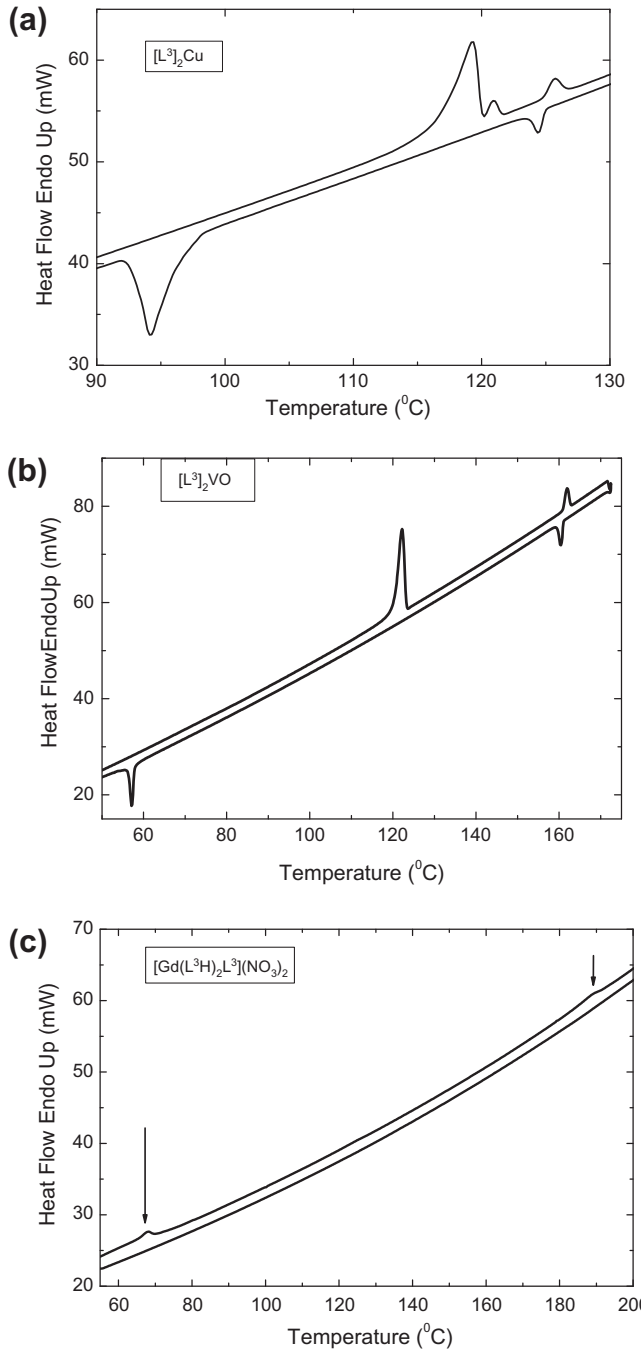

Fig. 9. (a) DSC spectrum of the compound **3-Cu**, (b) DSC spectrum of the compound **3-VO**, (c) DSC spectrum of the compound **3-Gd**.

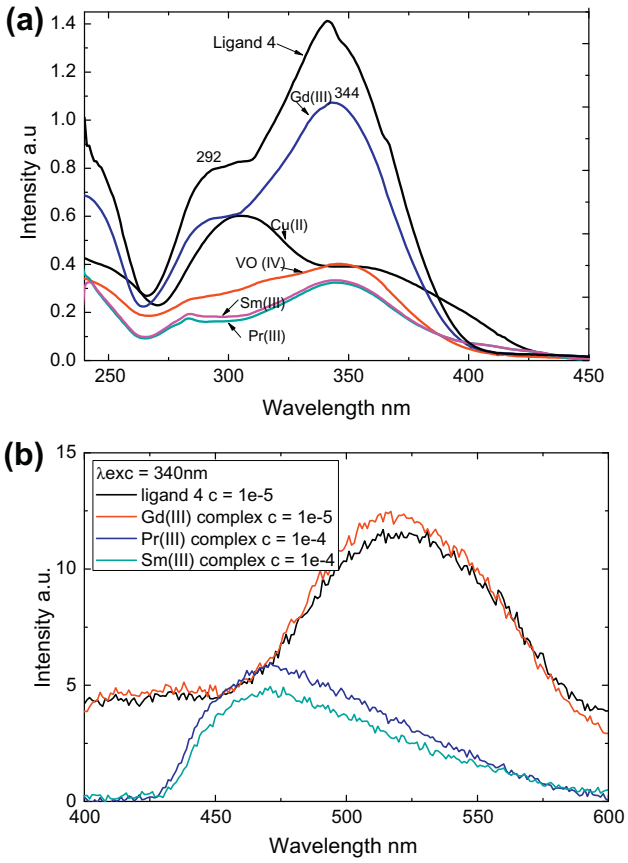

Fig. 10. (a) UV–Visible spectra of compound **4** and its Cu(II), VO(IV) and lanthanide complexes. (b) Fluorescence spectra of compound **4** and lanthanide complexes. Conc = 1×10^{-5} M.

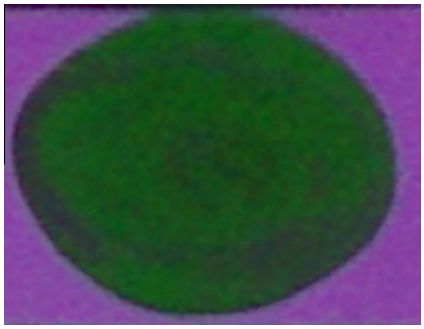

Fig. 11. Fluorescent image of **4-Gd** in solid state.

Table 5
UV–Visible data for the compound **4** and its complexes. (First row indicates the absorption wavelength in nm and second row indicates the molar extinction coefficient L mol^{-1} cm^{-1}.)

4	4-Cu	4-VO	4-Gd	4-Sm	4-Pr
245		234	237	241	
82,000		34,300	68,600	32,600	
300	302	284	292	282	283
81,300	59,900	25,500	58,700	18,800	17,500
		312			
		32,900			
345	355	346	344	344	343
133,800	39,100	39,900	107,300	33,400	32,400

References

[1] J.L. Serrano (Ed.), Metallomesogens, Synthesis, Properties and Applications, VCH, Weinheim, Germany, 1996.
[2] A.M. Giroud-Godquin, Metal-containing liquid crystals, in: D. Demus, J.W. Goodby, G.W. Gray, H.W. Spiess, V. Vill (Eds.), Handbook of Liquid Crystals, vol. IIB, Wiley-VCH, Weinheim, Germany, 1998, pp. 901–932.
[3] A.M. Giroud-Godquin, P.M. Maitlis, Angew. Chem. Int. Edit. Engl. 30 (1991) 375.
[4] P. Espinet, M.A. Esteruelas, L.A. Oro, J.L. Serrano, E. Sola, Coordin. Chem. Rev. 117 (1992) 215.
[5] D.W. Bruce, in: D.W. Bruce, D. O'Hare (Eds.), Inorganic Materials, second ed., Wiley, Chichester, 1996, pp. 405–490, (Chapter 8).
[6] D.W. Bruce, J. Chem. Soc. Dalton Trans. (1993) 2983.
[7] A.P. Polishchuk, T.V. Timofeeva, Russ. Chem. Rev. 62 (1993) 291.
[8] S.A. Hudson, P.M. Maitlis, Chem. Rev. 93 (1993) 861.
[9] L. Oriol, J.L. Serrano, Adv. Mater. 7 (1995) 348.
[10] N. Hoshino, Coordin. Chem. Rev. 174 (1998) 77.
[11] B. Donnio, D.W. Bruce, Struct. Bond. 95 (1999) 193–247.
[12] B. Donnio, D. Guillon, R. Deschenaux, D.W. Bruce, in: J.A. McCleverty, T.J. Meyer (Eds.), Comprehensive Coordination Chemistry II: From Biology to Nanotechnology, vol. 7, Elsevier, Oxford, UK, 2003, pp. 357–627.
[13] D.W. Bruce, R. Deschenaux, B. Donnio, D. Guillon, in: R.H. Crabtree, D.M.P. Mingos (Eds.), Comprehensive Organometallic Chemistry III, vol. 12, Elsevier, Oxford, UK, 2007, pp. 195–293. Chapter 12.05.
[14] Y.G. Galyametdinov, G.I. Ivanova, I.V. Ovchinnikov, Bull. Acad. Sci. USSR Div. Chem. Sci. 40 (1991) 1109.
[15] K. Binnemans, C. Gorller-Walrand, Chem. Rev. 102 (2002) 2303.
[16] K. Binnemans, Yu.G. Galyametdinov, R. Van Deun, D.W. Bruce, S.R. Collinson, A.P. Polishchuk, I. Bikchantaev, W. Haase, A.V. Prosvirin, L. Tinchurina, I. Litvinov, A. Gubajdullin, A. Rakhmatullin, K. Uytterhoeven, L. Van Meervelt, J. Am. Chem. Soc. 122 (2000) 4335.
[17] K. Binnemans, D.W. Bruce, S.R. Collinson, R. Van Deun, Yu.G. Galyametdinov, F. Martin, Phil. Trans. Roy. Soc. Lond. A357 (1999) 3063.
[18] E. Terazzi, S. Suarez, S. Torelli, H. Nozary, D. Imbert, O. Mamula, J.P. Rivera, E. Guillet, J.M. Benech, G. Bernardinelli, R. Scopelliti, B. Donnio, D. Guillon, J.C.G. Bunzli, C. Piguet, Adv. Funct. Mater. 16 (2006) 157.
[19] C. Piguet, J.C.G. Bunzli, Chem. Soc. Rev. 28 (1999) 347.
[20] J.C.G. Bunzli, Acc. Chem. Res. 39 (2006) 53.
[21] J.C.G. Bunzli, C. Piguet, Chem. Rev. 102 (2002) 1897;
J.C.G. Bunzli, C. Piguet, Chem. Soc. Rev. 34 (2005) 1048.
[22] A. Bellusci, G. Barberio, A. Crispini, M. Ghedini, M. La Deda, D. Pucci, Inorg. Chem. 44 (2005) 1818.
[23] T. Cardinaels, K. Driesen, I.N.P. Vogt, B. Heinrich, C. Bourgogne, D. Guillon, B. Donnio, K. Binnemans, Chem. Mater. 17 (2005) 6589.
[24] N.V.S. Rao, M.K. Paul, T.R. Rao, A. Prasad, Liq. Cryst. 29 (2002) 1243.
[25] N.V.S. Rao, T.D. Choudhury, R. Deb, M.K. Paul, T.R. Rao, T. Francis, I.I. Smalyukh, Liq. Cryst. 37 (2010) 1393.
[26] F. Martin, S.R. Collinson, D.W. Bruce, Liq. Cryst. 27 (2000) 859.
[27] W.J. Geary, Coordin. Chem. Rev. 7 (1971) 81.
[28] R.L. Farmer, F.L. Urbach, Inorg. Chem. 13 (1974) 587.
[29] M. Pasquali, F. Marchetti, S. Merlino, J. Chem. Soc., Dalton Trans. (1977) 139.
[30] A. Serrete, J. Carroll, T.M. Swager, J. Am. Chem. Soc. 114 (1992) 1887.
[31] E. Campillos, M. Marcos, A. Omenat, J.L. Serrano, J. Mater. Chem. 6 (1996) 349.
[32] S. Kumari, A.K. Singh, K.R. Kumar, B. Sridhar, T.R. Rao, Inorg. Chim. Acta 362 (2009) 4205.
[33] I.V. Ovchinnikov, Y.G. Galyametdinov, G.I. Ivanova, L.M. Yagfarova, Dokl. Akad. Nauk. SSSR 276 (1984) 126.
[34] Y.G. Galyametdinov, G.I. Ivanova, Izv. Akad. Nauk. SSSR, Ser. Khim. 9 (1989) 1997.
[35] Y.G. Galyametdinov, G.I. Ivanova, Izv. Akad. Nauk. SSSR, Ser. Khim. 12 (1989) 2833.
[36] K. Binnemans, J. Mater. Chem. 19 (2009) 448.
[37] D. Pucci, G. Barberio, A. Bellusci, A. Crispini, B. Donnio, L. Giorgini, M. Ghedini, M.L. Deda, E.I. Szerb, Chem. Eur. J. 12 (2006) 6738.
[38] R. Bayon, S. Coco, P. Espinet, Chem. Eur. J. 11 (2005) 1079.
[39] J. Arias, M. Bardaji, P. Espinet, Inorg. Chem. 47 (2008) 3559.
[40] H. Gallardo, R. Cristiano, A.A. Vieira, R.A.W. Neves Filho, R.M. Srivastava, I.H. Bechtold, Liq. Cryst. 35 (2008) 857.
[41] A.A. Vieira, R. Cristiano, A.J. Bortoluzzi, H.J. Gallardo, Mol. Struct. 875 (2008) 364.
[42] R.M. Srivastava, R.A.W.N. Filho, R. Schneider, A.A. Vieira, H. Gallardo, Liq. Cryst. 35 (2008) 737.
[43] R. Cristiano, F. Ely, H. Gallardo, Liq. Cryst. 32 (2005) 15.
[44] A.A. Vieira, R. Cristiano, F. Ely, H. Gallardo, Liq. Cryst. 33 (2006) 381.
[45] C.K. Lai, Y. Leu, Liq. Cryst. 25 (1998) 689.
[46] N.V.S. Rao, T.D. Choudhury, M.K. Paul, T. Francis, Liq. Cryst. 36 (Suppl.) (2009) 409.
[47] P. Keller, L. Liebert, Solid State Phys. 14 (1978) 19.
[48] M. Artigas, M. Marcos, E. Melendez, J.L. Serrano, Mol. Cryst. Liq. Cryst. 130 (1985) 337.